DISSERTATIONES SCHOLAE DOCTORALIS AD SANITATEM INVESTIGANDAM
UNIVERSITATIS HELSINKIENSIS

MIKAEL JUMPPANEN

# SYNTHESIS AND SAR ANALYSIS OF GATA4—NKX2-5 INTERACTION INHIBITORS WITH ANTIHYPERTROPHIC ACTIVITY

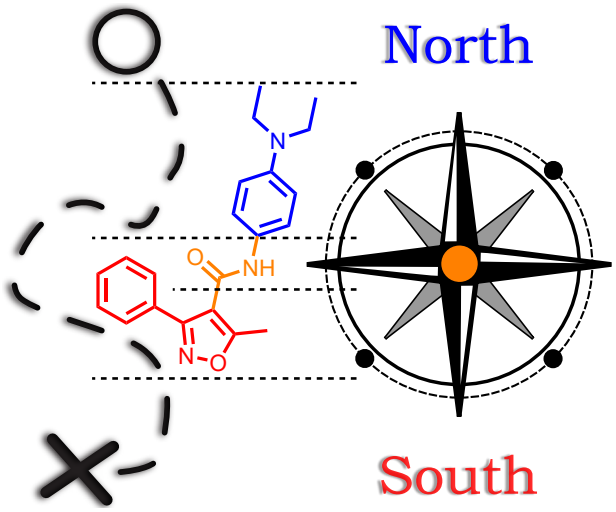


DRUG RESEARCH PROGRAM
DIVISION OF PHARMACEUTICAL CHEMISTRY AND TECHNOLOGY
FACULTY OF PHARMACY
DOCTORAL PROGRAMME IN DRUG RESEARCH
UNIVERSITY OF HELSINKI

Drug Research Program
Division of Pharmaceutical Chemistry and Technology
Faculty of Pharmacy
University of Helsinki
Finland

# SYNTHESIS AND SAR ANALYSIS OF GATA4-NKX2-5 INTERACTION INHIBITORS WITH ANTIHYPERTROPHIC ACTIVITY

**Mikael Jumppanen**

ACADEMIC DISSERTATION

To be presented, with the permission of the Faculty of Pharmacy of the University of Helsinki, for public examination in Lecture Hall 1041, Biocenter 2, on 5th of June 2020, at 2 pm.

Helsinki 2020

**Supervised by**

Dr. Gustav Boije af Gennäs
Drug Research Program
Division of Pharmaceutical Chemistry and Technology
Faculty of Pharmacy
University of Helsinki
Helsinki, Finland

Professor Jari Yli-Kauhaluoma
Drug Research Program
Division of Pharmaceutical Chemistry and Technology
Faculty of Pharmacy
University of Helsinki
Helsinki, Finland

**Reviewed by**

Professor Jens Hasserodt
Chemistry Laboratory
University of Lyon—Ecole Normale Supérieure de Lyon
Lyon, France

Professor Outi Salo-Ahen
Faculty of Science and Engineering, Pharmacy
Åbo Akademi University
Turku, Finland

**Opponent**

Professor Stephan Schürer
Department of Molecular and Cellular Pharmacology
Miller School of Medicine
University of Miami
Miami
Florida, USA

Dissertationes Scholae Doctoralis Ad Sanitatem Investigandam Universitatis Helsinkiensis

© Mikael Jumppanen 2020
ISBN 978-951-51-6181-9 (paperback)
ISBN 978-951-51-6182-6 (PDF)
ISSN 2342-3161 (print)
ISSN 2342-317X (online)

Unigrafia
Helsinki 2020

# ABSTRACT

Cardiac disease continues to be a leading cause of death and hospitalizations in developed countries. Transcription factors GATA4 and NKX2-5 are master regulators of cardiac gene expression, taking part in multiple processes during heart development, as well as hypertrophy and recovery after e.g. myocardial infarction.

Pathological hypertrophy is a homeostatic process, which often leads to cardiac dysfunction in pathological conditions (e.g. hypertension, genetic alterations, and myocardial infarction) further progressing to heart failure.

There is an urgent need for treatments that would prevent disease progression at a molecular level. To date, no therapies have directly targeted the transcriptional regulation of cardiac hypertrophy. A novel treatment for this target would be particularly interesting, as current treatments are slowing the disease progression without directly targeting hypertrophic gene expression.

The aim of this thesis was to design and synthesize nontoxic GATA4-NKX2-5 interaction inhibitors with antihypertrophic activity and determine their mechanism of action. Furthermore, the generated luciferase and toxicity assay data were analyzed to select compounds for further evaluation. In addition, different cycloaddition methods were explored for a facile synthesis of isoxazole scaffold. Finally, the mechanism of action of the original hit compound **1** was validated with affinity chromatography.

In conclusion, novel inhibitors of GATA4-NKX2-5 transcriptional synergy were identified, which inhibit hypertrophic gene expression in rat cardiomyocytes. Remarkably, the immobilized hit compound (**1**) was shown to bind to GATA4 in the target validation study. In addition, with hierarchical clustering, a group of synergy inhibitors were identified that did not inhibit GATA4 transcriptional activity at 3 μM concentration. Further studies to determine the therapeutic potential of these more selective compounds are clearly needed.

# TIIVISTELMÄ

Sydänsairaudet ovat merkittävin kuolinsyy ja syy lisääntyneisiin sairaalapäiviin teollisuusmaissa. Transkriptiotekijät GATA4 ja NKX2-5 säätelevät sydängeenien ilmentymistä ja osallistuvat moniin prosesseihin, jotka liittyvät sydämen kehittymiseen, liikakasvuun ja esimerkiksi sydäninfarktin jälkeiseen toipumiseen.

Patologinen liikakasvu on homeostaattinen prosessi, joka johtaa usein toimintahäiriöihin sydämen patologisissa tiloissa (esim. verenpainetauti, geneettiset muutokset ja sydäninfarkti) edeten sydämen vajaatoimintaan.

Tulevaisuudessa on suuri tarve hoitomuodoille, jotka hidastavat taudin etenemistä molekyylitasolla. Nykyiset sydämen liikakasvun hoitomuodot eivät kohdistu suoraan sydämessä tapahtuvan transkription säätelyyn. Uusi hoitomuoto tähän kohteeseen olisi erityisen mielenkiintoinen, koska nykyiset hoitomuodot hidastavat sairauden etenemistä mutta eivät suoraan vaikuta sydämen liikakasvuun johtavien geenien ilmentymiseen.

Tämän väitöskirjatyön tavoitteena oli suunnitella ja valmistaa sydämen liikakasvua vähentäviä GATA4:n ja NKX2-5:n välisen vuorovaikutuksen estäjiä, jotka eivät olisi toksisia, sekä todentaa niiden vaikutusmekanismi. Lusiferaasi- ja toksisuusdata analysoitiin, jotta voitaisiin valita yhdisteitä jatkotutkimuksiin. Tämän lisäksi tutkittiin erilaisia sykloadditioreaktiota isoksatsolirakenteisen molekyylirungon valmistamiseen. Lopuksi alkuperäisen hit-yhdisteen **1** vaikutusmekanismi validoitiin käyttämällä molekyylibiologisia menetelmiä ja affiniteettikromatografiaa.

Tässä väitöskirjatyössä tunnistettiin uusia GATA4:n ja NKX2-5:n transkriptiosynergiaan vaikuttavia isoksatsolirakenteisia yhdisteitä, jotka estävät rotan kardiomyosyyttien liikakasvuun johtavien geenien ilmentymistä. Merkittävä löytö oli se, että hit-yhdiste (**1**) sitoutui GATA4:ään biologisen vaikutuskohteen validointitutkimuksessa. Hyödyntäen hierarkista klusterointia voitiin lisäksi tunnistaa joukko synergiaestäjiä, jotka eivät estäneet GATA4:n transkriptioaktiivisuutta, kun yhdisteiden pitoisuus oli 3 μM. Lisätutkimuksia tarvitaan, jotta voitaisiin arvioida näiden aiempaa selektiivisempien yhdisteiden toimivuutta mahdollisissa lääkehoidoissa.

# ACKNOWLEDGEMENTS

This work was carried out at the Division of Pharmaceutical Chemistry and Technology, Faculty of Pharmacy University of Helsinki, during the years of 2015-2020. I would like to acknowledge Vilho, Yrjö and Kalle Väisälä Foundation of the Finnish Academy of Science and Letters for funding final months of my doctoral studies.

First of all, I would like to thank my supervisors Dr. Gustav Boije af Gennäs and prof. Jari Yli-Kauhaluoma for trusting me in the first place and taking me in to your group. Your enthusiasm and love for science have been truly encouraging. Gusse your positivity was always inspiration for me, especially in the first stage of my Phd journey. You always find a way to get forward with any problem. Jari, you have been very supportive through this journey, and your door is always open for any kind of questions and problems.

Further, I would like to thank all the members of the 3iRegeneration project, and especially 3iheart group. Prof. Heikki Ruskoaho you always know how to encourage, and that has been personally very important during these years. I am grateful to you for reading and commenting my Phd thesis (and all the other texts). Dr. Virpi Talman, I am truly grateful to you for comments regarding manuscripts, conference abstracts, posters and reports. I also want to acknowledge other members of the project team: Sini Kinnunen, Matej Zore, Samuli Auno, Tuuli Karhu, Lotta Pohjalainen, Mika Välimäki, Henri Xhaard, Vigneshwari Subramanian, Maiju Rinne and Ingo Aumüller. This thesis would have not been possible without your contribution. Ingo, especially your contribution regarding the *J. Med. Chem.* paper was remarkable (~200 synthesized compounds), I also appreciate deep discussions, which improved the quality of the article to even higher level.

Special thanks go to Laura Kolsi, who was my "spy" in JYK-group when I was planning to apply there. We both studied at the same time in Aalto University where we both did our Master's degree. Your friendship and support was essential during this Phd journey. I would like to express my gratitude to all current and past members of the JYK-group, especially Teppo, Tiina, Niklas, Riky, Tanja, Andrew, Ghada, Henri, Erik, Alexi, Ralica, Jayendra, Piyush, Raisa, Leena, Paula, Mikko as well as other collegues at the Faculty of Pharmacy, especially Kati, Erkka, Ainoleena and Katja.

I also want to thank my family and friends for their support during this journey. I want to thank especially my friends Daniel and Pyry who share the same passion for science, we have had a lot of discussions about science and other more important topics of life.

Helsinki, May 2020

Mikael Jumppanen

*The Road goes ever on and on*
*Down from the door*
*where it began.*
*Now far ahead*
*the Road has gone,*
*And I must follow,*
*if I can,*
*Pursuing it with eager feet,*
*Until it joins some larger way*
*Where many paths and errands meet.*
*And whither then?*
*I cannot say.*

***Bilbo Baggins in The Fellowship of the Ring (1954)***

# CONTENTS

Abstract ..... iii

Tiivistelmä ..... iv

Acknowledgements ..... v

Contents ..... vii

List of original publications ..... ix

Abbreviations ..... xii

1 Introduction ..... 1

2 Review of the literature ..... 3

2.1 Cardiac hypertrophy ..... 3

2.1.1 Biological pathways in cardiac hypertrophy ..... 4

2.1.2 Transcription factors GATA4 and NKX2-5 in hypertrophy ..... 7

2.1.3 Compounds targeting GATA4 and NKX2-5 transcriptional synergy ..... 8

2.2 [3+2] Dipolar cycloaddition reactions for synthesis of the isoxazole core ..... 9

2.2.1 Reaction mechanism and regiochemistry ..... 10

2.2.2 Reactions and synthesis ..... 11

2.3 Toxicity mechanisms of different ring systems ..... 12

2.3.1 Cytochrome P450 metabolism ..... 12

2.3.2 Stacking interactions of rings in drugs ..... 14

2.3.3 DNA intercalation ..... 15

2.4 Target identification with affinity chromatography ..... 15

3 Aims of the study ..... 19

4 Results and discussion ..... 20

4.1 Synthesis of 3,4,5-trisubstituted isoxazole derivatives (Publications I & II) ..... 20

4.2 Scaffold hopping (Publication II) ..... 21
4.3 SAR analysis (Publication II) ..... 23
4.3.1 Southern part ..... 24
4.3.2 Central part ..... 27
4.3.3 Northern part ..... 28
4.4 Cytotoxicity (Publication II) ..... 31
4.5 Data analysis (Publication II) ..... 33
4.6 Antihypertrophic activity (Publication II) ..... 39
4.7 Target validation with affinity chromatography (Publ. III) ... 40
4.7.1 Synthesis ..... 41
4.7.2 Biological testing ..... 42
5 Summary and conclusions ..... 44
References ..... 46

# LIST OF ORIGINAL PUBLICATIONS

This thesis is based on the following publications referred to in the text by their Roman numerals:

I Karhu, S.T., Välimäki, M.J., **Jumppanen, M.**, Kinnunen, S.M., Pohjolainen, L., Leigh, R.S., Auno, S., Földes, G., Boije af Gennäs, G., Yli-Kauhaluoma, J., Ruskoaho, H. and Talman, V. Stem cells are the most sensitive screening tool to identify toxicity of GATA4-targeted novel small-molecule compounds. *Archives of Toxicology*, **2018**, *92* (9), 2897-2911.

The supporting information with detailed materials and methods: https://static-content.springer.com/esm/art%3A10.1007%2Fs00204-018-2257-1/MediaObjects/204_2018_2257_MOESM1_ESM.pdf

II **Jumppanen, M.**, Kinnunen, S.M., Välimäki, M.J., Talman, V., Auno, S., Bruun, T., Boije af Gennäs, G., Xhaard, H., Aumüller, I.B., Ruskoaho, H. and Yli-Kauhaluoma, J. Synthesis, Identification, and Structure–Activity Relationship Analysis of GATA4 and NKX2-5 Protein–Protein Interaction Modulators. *Journal of Medicinal Chemistry*, **2019**, *62* (17), 8284-8310.

The supporting information with detailed materials and methods: https://pubs.acs.org/doi/suppl/10.1021/acs.jmedchem.9b01086/suppl_file/jm9b01086_si_001.pdf

III **Jumppanen, M.***, Zore, M.*, Kinnunen, S.M.*, Välimäki, M.J., Talman, V., Boije af Gennäs, G., Ruskoaho, H.J., Yli-Kauhaluoma, J. Affinity chromatography reveals a direct binding of the GATA4-NKX2-5 interaction inhibitor (**3i-1000**) with GATA4. *Submitted*.

The supporting information with detailed materials and methods is available from the author.

Authors' contributions:

I MJ synthesized and characterized part of the compounds, and prepared synthetic chemistry sections of the manuscript. MJV carried out the computational part of the study. STK carried out pharmacological part of the study.

II MJ synthesized and characterized part of the compounds, and prepared the manuscript with contributions of all authors. SAR analysis of all prepared compounds was conducted by MJ.

III MJ contributed in planning of the study. MJ synthesized and characterized all compounds together with MZ. SK conducted biological part of the study together with MZ. MZ worked in the laboratory under supervision of MJ and SK. MJ, SK and MZ prepared the manuscript with equal contribution.

Publication I is included in the dissertation of Mika Välimäki (MJV) and will be included in the dissertation of Tuuli Karhu (STK). Publication III will be included in the dissertation of Sini Kinnunen (SK).

Additional publications:

Kauko, O., Laajala, T.D.; **Jumppanen, M.**, Hintsanen, P., Suni, V., Haapaniemi, P., Corthals, G., Aittokallio, T., Westermarck, J., Imanishi, S.Y. Label-Free Quantitative Phosphoproteomics with Novel Pairwise Abundance Normalization Reveals Synergistic RAS and CIP2A Signaling. *Sci. Rep.* **2015**, *5*, 13099. https://doi.org/10.1038/srep13099.

Laajala, T.D., **Jumppanen, M.**, Huhtaniemi, R., Fey, V., Kaur, A., Knuuttila, M., Aho, E., Oksala, R., Westermarck, J., Mäkelä, S., Poutanen, M., Aittokallio, T. Optimized Design and Analysis of Preclinical Intervention Studies in Vivo. *Sci. Rep.* **2016**, *6*, 30723. https://doi.org/10.1038/srep30723.

Kaur, A., Denisova, O.V., Qiao, X., **Jumppanen, M.**, Peuhu, E., Ahmed, S.U., Raheem, O., Haapasalo, H., Eriksson, J., Chalmers, A.J., Laakkonen, P., Westermarck, J. PP2A Inhibitor PME-1 Drives Kinase Inhibitor Resistance in Glioma Cells. *Cancer Res.* **2016**, *76* (23), 7001–7011. https://doi.org/10.1158/0008-5472.CAN-16-1134.

Zhang, Y.*, **Jumppanen, M.***, Maksimainen, M.M., Auno, S., Awol, Z., Ghemtio, L., Venkannagari, H., Lehtiö, L., Yli-Kauhaluoma, J., Xhaard, H., Boije af Gennäs, G. Adenosine Analogs Bearing Phosphate Isosteres as Human MDO1 Ligands. *Bioorg. Med. Chem.* **2018**, *26* (8), 1588–1597. https://doi.org/10.1016/j.bmc.2018.02.006.

Mattila, A., Andsten, R.-M., **Jumppanen, M.**, Assante, M., Jokela, J., Wahlsten, M., Mikula, K.M., Sigindere, C., Kwak, D.H., Gugger, M.; Koskela, H., Sivonen, K., Liu, X., Yli-Kauhaluoma, J., Iwaï, H., Fewer, D. Biosynthesis of the Bis-Prenylated Alkaloids Muscoride A and B. *ACS Chem. Biol.* **2019**, *14* (12), 2683–2690. https://doi.org/10.1021/acschembio.9b00620.

Kinnunen, S., Tölli, M., Välimäki, M., **Jumppanen, M.**, Boije af Gennäs, G., Yli-Kauhaluoma, J., Ruskoaho, H. Isoxazole-amides for treating cardiac diseases. PCT Int. Appl. WO2018/055235 A1, **2018**.

# ABBREVIATIONS

| | |
|---|---|
| α/β-AR | α- or β-adrenergic receptor |
| AC | adenylyl cyclase |
| ACE | angiotensin converting enzyme |
| AKT | RAC-alpha serine/threonine-protein kinase |
| AT-R | angiotensin II receptor |
| BNP | B-type natriuretic peptide |
| BOC | *tert*-butoxycarbonyl |
| BRD4 | bromodomain-containing protein 4 |
| CYP | cytochrome P450 |
| DFT | density functional theory |
| DHODH | human dihydroorotate dehydrogenase |
| DIB | (diacetoxy)iodobenzene |
| DIPEA | *N,N*-diisopropylethylamine |
| DMF | *N,N*-dimethylformamide |
| Endo-R | endothelin 1 receptor |
| ERG | electron releasing group |
| ERK1/2 | extracellular signal-regulated kinases ½ |
| ET-1 | endothelin-1 |
| EWG | electron withdrawing group |
| FMO | frontier molecular orbital |
| FTIR | Fourier-transform infrared spectroscopy |
| GATA4 | GATA binding protein 4 |
| GHS-R | growth hormone secretagogue receptor |
| GPCR | G-protein coupled receptor |
| GSH | glutathione |
| HATU | 1-[bis(dimethylamino)methylene]-1*H*-1,2,3-triazolo[4,5-*b*]pyridinium 3-oxide hexafluorophosphate |
| HBTU | *N,N,N′,N′*-tetramethyl-*O*-(1*H*-benzotriazol-1-yl)uronium hexafluorophosphate |
| HOMO | highest occupied molecular orbital |
| HTIB | [hydroxy(tosyloxy)iodo)]benzene |
| IGF1 | insulin-like growth factor 1 |
| IR | tyrosine kinase insulin receptor |
| JNK | c-Jun N-terminal kinase |
| LDH | lactate dehydrogenase |
| LUMO | lowest unoccupied molecular orbital |
| MAPK | mitogen-activated protein kinase |
| MAPKK | MAPK kinase |
| MAPKKK | MAPK kinase kinase |
| MEF2 | myocyte enhancer factor 2 |
| MEK1 | mitogen-activated protein kinase kinase 1 |

| | |
|---|---|
| MMP | matrix metalloproteinase |
| MO | molecular orbital |
| MTT | 3-(4,5-dimethylthiazol-2-yl)-2,5-diphenyltetrazolium |
| MYH6 | myosin heavy chain 6 |
| MYH7 | myosin heavy chain 7 |
| NFAT | nuclear factor of activated T cells |
| NFκB | nuclear factor kappa-light-chain-enhancer of activated B cells |
| NKX2-5 | NK2 homeobox 5 |
| PDGF | platelet-derived growth factor |
| PEG | polyethyleneglycol |
| PI3K | phosphoinositide 3-kinase |
| PKA | protein kinase A |
| PTEN | phosphatase and tensin homolog |
| SAR | structure-activity relationship |
| SDS-PAGE | sodium dodecyl sulfate polyacrylamide gel electrophoresis |
| $T_3$ | thyroid hormone |
| TFA | trifluoroacetic acid |
| VEGFB | vascular endothelial growth factor B |
| VEGFR1 | vascular endothelial growth factor receptor 1 |

# 1 INTRODUCTION

Reptiles, birds and mammals have hearts with two atrial and two ventricular chambers, unlike the hearts of simpler organisms, such as fishes, which have a single atrium and ventricle.[1] The main function of the heart is to provide oxygenated blood around the body. Interestingly, it seems that oxygen causes cardiac cell cycle arrest and inhibition of proliferative capacity.[2] This explains why animals such as zebrafish and neonatal mice retain regenerative capacity in their hearts that have lower oxygen levels, but the hearts of adult mice, for example, that have a higher oxygen level, do not regenerate. Remarkably, there are case reports of complete recovery of human neonatal hearts after severe myocardial infarction.[3–5] Regenerative inability is especially devastating in pathological conditions such as myocardial infarction in which millions to billions of cells are lost. Myocardial infarction often leads to heart failure, in fact, it is a underlying etiology in 70% of heart failure cases.[6] One of the main routes to heart failure after myocardial infarction is through hypertrophy, remodeling and dilatation of non-infarcted myocardium.[7]

Clinically used and future therapies for myocardial infarction can be classified based on their target regions during left ventricular remodeling (**Table 1**).[7] During the subacute phase, it is crucial to prevent infarct expansion.[7] Interestingly, it has been observed that an expansion is directly proportional to the number of heart beats,[7] which rationalizes the use of β-blockade at this stage. Each contraction (during the heart beat) contributes to left ventricular remodeling through increased wall stress.[7] Wall stress can be decreased, for example, by lowering the blood pressure with angiotensin converting enzyme (ACE) inhibitors or with intravenous nitroglycerin, which reduces left ventricular filling pressure.[7,8] In addition, nitroglycerin improves perfusion to borderline areas of the infarction.[8] Improved perfusion is probably due to dilated epicardial coronary arteries.[9]

In the following weeks to months, viable cells adjacent to the infarct scar may undergo apoptosis due to mechanical stress.[7] Preclinical studies have proposed that current standard care (ACE inhibition and β-blockade) limits nonischemic infarct extension at this stage.[7]

Beyond the adjacent region lies the remote non-infarcted region that is unaffected by myocardial infarction in the early phase.[7] However, increased workload due to large myocardial infarction can induce hypertrophic response in the remote region. Based on the fact that hypertrophic response is induced by wall stress, it is unsurprising that ACE inhibitors and β-blockade have beneficial effect also at this stage. In addition, mineralocorticoid receptor blockers (aldosterone receptor antagonists) have been shown to be effective for inhibiting cardiac fibrosis and hypertrophy in a chronic phase.[10]

There is an urgent need for treatments that can prevent disease progression at a molecular level. Recent advances have shed light upon the transcriptional

regulation of cardiac hypertrophy,[11,12] yet no therapies have been developed to directly target this process. A novel treatment targeting this process would be particulary interesting, as current treatments slow disease progression without directly targeting hypertrophic gene expression.

Isoxazole is a five-membered heterocyclic structure found in many bioactive compounds.[13] Synthetic advances have promoted interest in isoxazoles in drug development settings, because controlling regiochemistry in dipolar cycloaddition reactions has become easier with various catalytic methods. In drug development, various aspects of the bioactive molecule need to be taken into account. Some compounds are toxic, insoluble, ineffective or have an non-specific mode of action. The obtained data have to be carefully analyzed to identify potential true hits for further validation. The clinical translatability of the preliminary assays and identification of the true target of the compound of interest are the most important individual factors in the drug development process.

In the following literature review, the biological rationale of the study is discussed regarding cardiac hypertrophy. In addition, synthetic methods to prepare isoxazoles are presented with a theory regarding the regiochemistry of the dipolar cycloaddition reactions. Next, possible toxicity mechanisms are discussed based on the molecular structures of the compounds.

In the results and discussion section, synthesis of the isoxazoles and compounds for affinity chromatography are presented together with a structure-activity relationship (SAR) analysis. Finally, results regarding the target validation study with affinity chromatography are presented.

**Table 1** Currently used and therapeutic strategies under development to treat myocardial infarction in different time frames after infarction and their targets in specific regions of the heart.[7] Abbreviations: ACE, angiotensin converting enzyme; MMP, matrix metalloproteinase.

| Heart region | Time frame | Current therapies | Developing therapies |
|---|---|---|---|
| **Infarct** | Days to weeks | Nitroglycerin | Better scar formation |
| | | ACE inhibition | MMP inhibition |
| | | β-blockade | Passive restraint |
| | | | Stem-cell transplantation |
| **Adjacent** | Weeks to months | ACE inhibition | Antiapoptosis |
| | | β-blockade | Anticytokine |
| | | | Passive restraint |
| | | | Anti-inflammatory |
| **Remote** | Months to years | ACE inhibition | Antihypertrophy |
| | | β-blockade | Anticytokine |
| | | Aldosterone inhibition | MMP inhibition |

# 2 REVIEW OF THE LITERATURE

## 2.1 CARDIAC HYPERTROPHY

Cardiac hypertrophy can be divided into physiological and pathophysiological forms. Pathological cardiac hypertrophy can be seen as an intermediate step enroute to heart failure.[14] It is an adaptive process to normalize wall stress of the left ventricle in pathological conditions such as volume or pressure overload of the ventricle due to myocardial infarction or hypertension.[14] According to Laplace's law (**Equation 1**), wall stress of a sphere is directly proportional to the radius and pressure, and indirectly proportional to wall thickness. Pathological hypertrophy is characterized by thickening of the ventricular wall (concentric hypertrophy), dilatation of the ventricular chamber (eccentric hypertrophy), contractile dysfunction, and heart failure (**Figure 1**).[15] On the other hand, physiological hypertrophy is fully reversible and is characterized sometimes even by the improvement of contractile function.[15] Understanding the biological processes behind these conditions is crucial for the development of targeted therapeutics for reversing and preventing disease progression.

(1) $$WS = P \times \frac{R}{2T},$$

where

$WS$ = wall stress of a sphere (ventricle)
$P$ = pressure (ventricular)
$R$ = radius (of the chamber)
$T$ = wall thickness

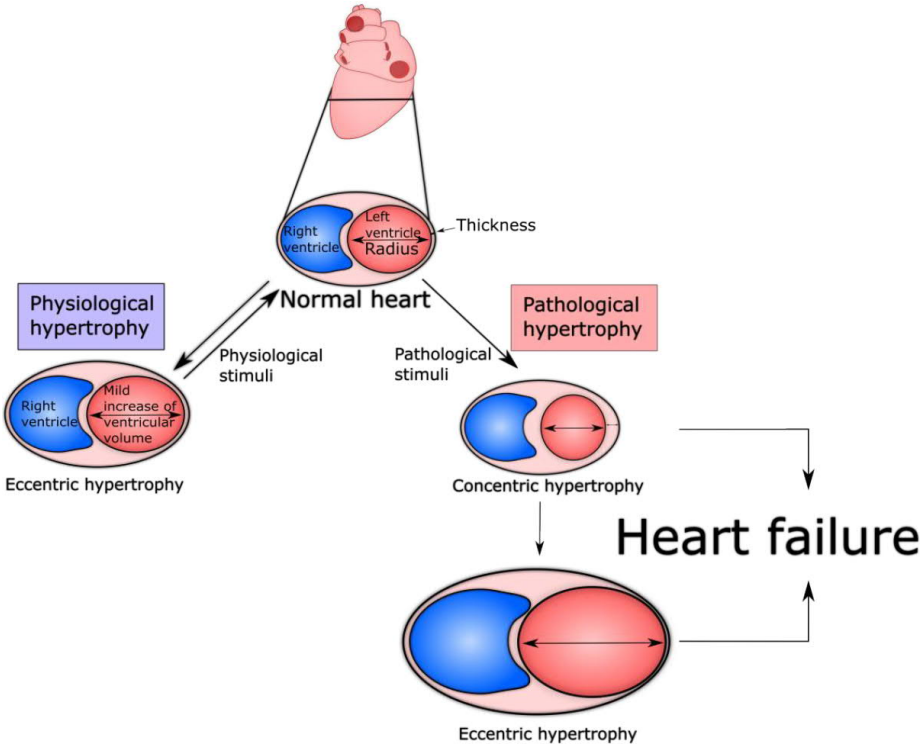


**Figure 1** Normal adult heart, physiological hypertrophy and pathological forms of hypertrophy (eccentric or concentric). Modified from ref 16.

### 2.1.1 BIOLOGICAL PATHWAYS IN CARDIAC HYPERTROPHY

Interestingly, physiological hypertrophy can reverse the progression of pathological hypertrophy to more severe conditions such as heart failure.[17] Physiological hypertrophy is induced by repetitive endurance exercise and pregnancy, for example.[15] The molecular mechanisms of physiological hypertrophy have been the focus of intense research.[16,18–20] Although many studies also mention cardiomyocyte proliferation due to exercise training, this concept has been challenged by other researchers[21–23] and later studies[24]. There has been ongoing debate[22,23] if cardiomyocytes divide in an adult heart. However, the consensus seems to be that cardiomyocytes do not divide in the adult heart to a large extent, but can undergo other cell-cycle variations leading to the formation of polyploid (two or more paired sets of chromosomes) cardiomyocytes and furthermore hypertrophy.[22,23]

Physiological hypertrophy is launched by signaling pathways active in cell growth, proliferation, survival, and angiogenesis. At the molecular level, insulin, insulin-like growth factor 1 (IGF1), thyroid hormone ($T_3$), vascular endothelial growth factor B (VEGFB), platelet-derived growth factor (PDGF),

nitric oxide, neuregulin 1 and periostin are endogenous ligands activating the hypertrophic pathways in a cell.[15] In the context of transcriptional regulation, the downstream signaling of $T_3$, VEGFB, insulin, and IGF1 are especially interesting.[16] Signaling pathways related to transcriptional regulation of physiological hypertrophy are presented in **Figure 2**. $T_3$ regulates gene transcription related to $Ca^{2+}$ handling by downregulating the expression of myosin heavy chain 7 (MYH7) and upregulating expression of myosin heavy chain 6 (MYH6). Insulin and IGF1 are involved in multiple cellular processes in the heart related to hypertrophy. Intracellular signaling related to gene transcription converges around nodal mediators such as phosphoinositide 3-kinase-phosphatase and tensin homolog (PI3K-PTEN), RAC-alpha serine/threonine-protein kinase (AKT), and extracellular signal-regulated kinases 1/2 (ERK1/2).[16] For example, exercise-induced physiological hypertrophy signaling leads to downregulation of transcription factor C/EBPβ through AKT1. C/EBPβ downregulates[25] other cardiac transcription factors such as GATA binding protein 4 (GATA4) and NK2 homeobox 5 (NKX2-5) and its knockdown[26] has been associated with hypertrophy inhibition via p65-nuclear factor kappa-light-chain-enhancer of activated B cells (p65-NFκB) signaling pathway.

Along with adaptive processes, cell growth, and protein synthesis, pathological hypertrophy is characterized by the following maladaptive hallmarks: cell death, fibrosis, dysregulation of $Ca^{2+}$ handling proteins, mitochondrial dysfunction, metabolic reprogramming, reactivation of fetal gene expression, impaired protein and mitochondrial quality control, altered sarcomere structure, and insufficient angiogenesis.[15] Calcium-calcineurin signaling during pathological hypertrophy is especially interesting as it directly regulates[27] transcription of the genes associated with pathological hypertrophy. Furthermore, mitogen-activated protein kinase (MAPK) signaling cascade is closely linked to transcriptional regulation of hypertrophic genes, such as GATA4 and myocyte enhancer factor 2 (MEF2), through p38 and c-Jun N-terminal kinase (JNK) branches.[28] Signaling pathways related to transcriptional regulation of maladaptive gene expression are presented in **Figure 3**.

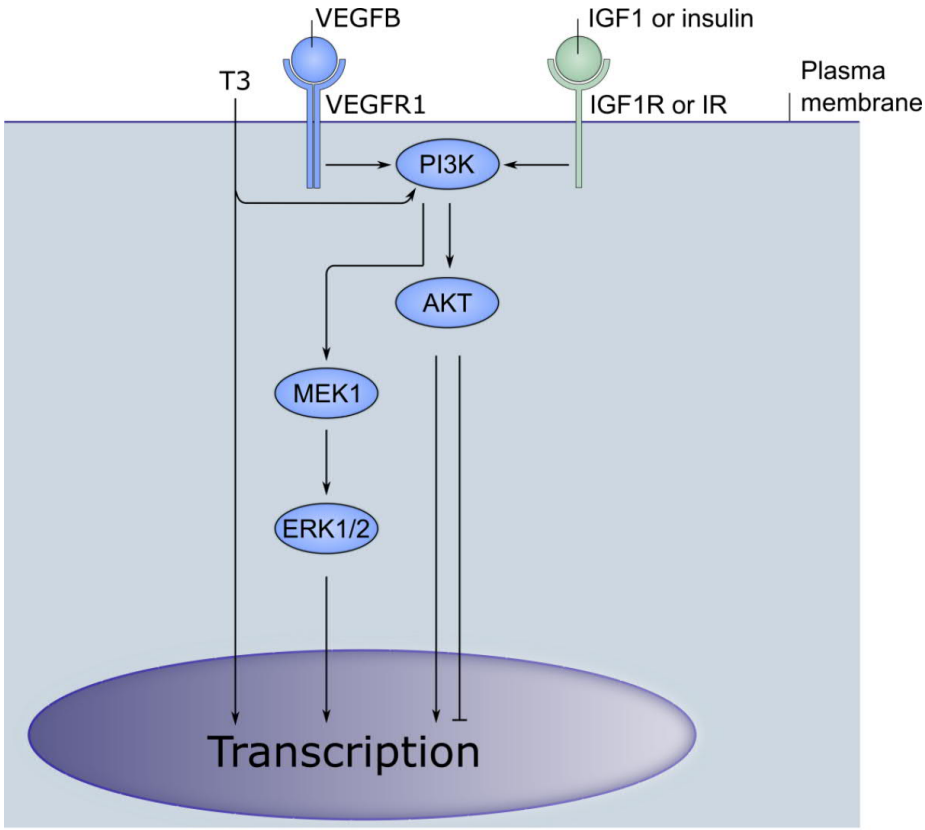


**Figure 2** Signaling pathways affecting gene transcription of physiological hypertrophy through endogenous ligands: VEGFB, T3, IGF1, or insulin. Abbreviations: AKT, RAC-alpha serine/threonine-protein kinase; ERK 1/2, extracellular signal-regulated kinases 1/2; IR, tyrosine kinase insulin receptor; MEK 1, mitogen-activated protein kinase kinase 1; PI3K, phosphoinositide 3-kinase; VEGFR1, vascular endothelial growth factor receptor 1. Modified from ref 16.

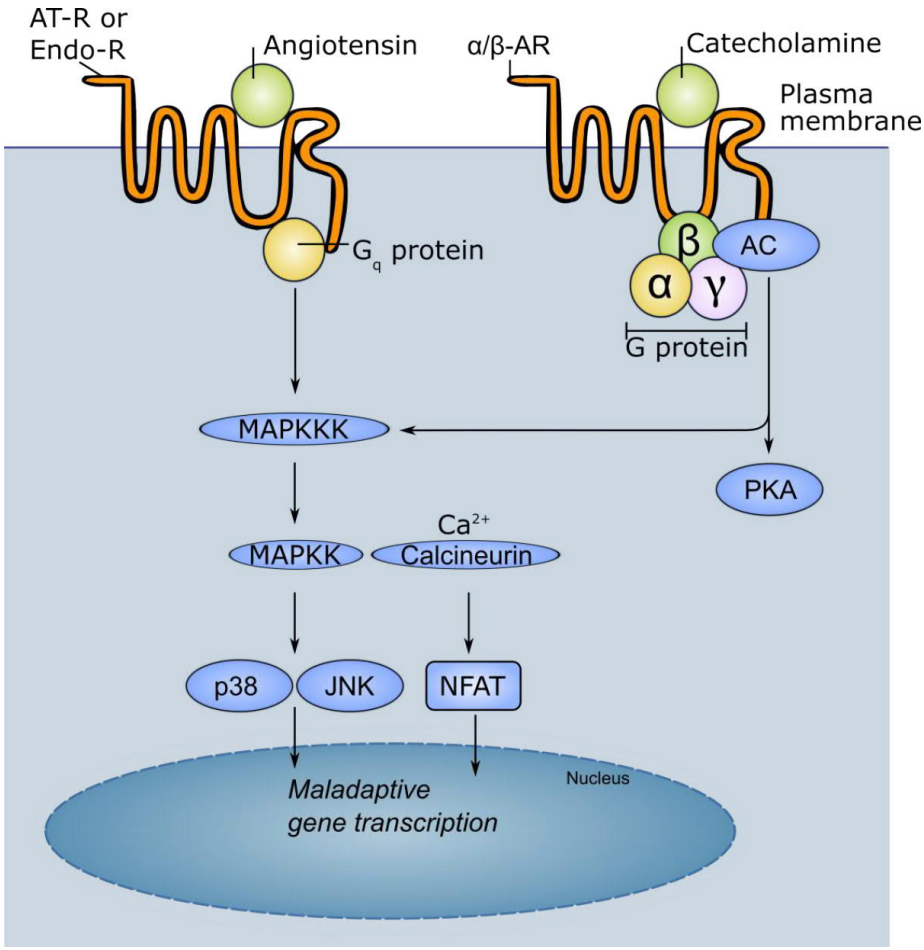


**Figure 3** Signaling pathways inducing maladaptive hypertrophic gene expression. Abbreviations: AC, adenylyl cyclase; AT-R, angiotensin II receptor; Endo-R, endothelin 1 receptor; α/β-AR, α- or β-adrenergic receptor; JNK, c-Jun N-terminal kinase; MAPKK, MAPK kinase; MAPKKK, MAPK kinase kinase; NFAT, nuclear factor of activated T cells; PKA, protein kinase A. Modified from ref 16.

### 2.1.2 TRANSCRIPTION FACTORS GATA4 AND NKX2-5 IN HYPERTROPHY

Transcription factors GATA4 and NKX2-5 are master regulators of cardiac gene expression. They are involved in multiple processes related to cell differentiation, cardiac hypertrophy, and disease progression.[29–31] GATA4 and NKX2-5 directly and synergistically interact with each other activating cardiogenic gene transcription.[32] Previous studies have shown that GATA4 mediates its pathological hypertrophic effect through physical interaction with other cardiac transcription factors such as NKX2-5[33] and through posttranslational[34] modifications.

Physical interaction between GATA4 and NKX2-5 is especially interesting as it has been shown to be essential for mechanical stretch-induced cardiomyocyte hypertrophy.[33] Furthermore, Pikkarainen et al.[33] showed that myocyte stretch activates BNP (B-type natriuretic peptide) transcription in a GATA4-dependent mechanism. BNP is a well-established biomarker[35,36] for heart disease, as well as increased mechanical load and wall stretch in the heart,[37] and its lower levels would indicate inhibition of stretch-induced hypertrophic signaling.

### 2.1.3 COMPOUNDS TARGETING GATA4 AND NKX2-5 TRANSCRIPTIONAL SYNERGY

Earlier studies[32,38] of GATA4 and NKX2-5 transcriptional synergy have reavealed hot spots of their protein-protein interaction. A further pioneering study of Välimäki et al.[39] showed that transcriptional synergy of GATA4 and NKX2-5 can be targeted by small molecular compounds, which either inhibit or enhance transcriptional synergy of GATA4 and NKX2-5. The initial hit compounds were identified by using a fragment-based screening and pharmacophore search. Chemical structures of some initial hit compounds are presented in **Figure 4**. The common structural feature for the initial hit compounds found in fragment-to-hit growth was a hydrogen bond acceptor (such as imine or amide) next to the five (or six)-membered ring. Compounds were tested in an iterative process using a luciferase reporter assay to measure GATA4 and NKX2-5 transcriptional synergy. The most promising compound **1** was tested in cytotoxicity, G-protein coupled receptor (GPCR), and kinase profiling assays to determine possible off-target effects. In addition, a small set of compounds was tested for possible molecular aggregation and compound **1** for chemical stability.

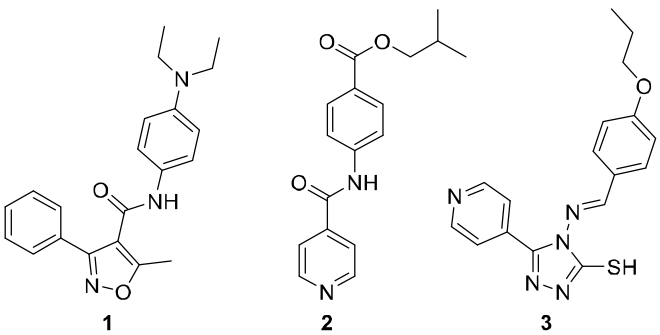


**Figure 4** Examples of the initial hit compounds targeting transcriptional synergy of GATA4 and NKX2-5.[39]

The luciferase assay measures the inhibition or enhancement of transcriptional synergy of GATA4 and NKX2-5.[38] The cell assay is based on ability of GATA4 and NKX2-5 to synergistically activate gene transcription (of luciferase enzyme) through the NXK2-5 binding site on DNA (**Figure 5**). Activation can be measured with a luminometer, which measures light emitting from the luciferase-catalyzed multistep reaction between D-luciferin, ATP, molecular oxygen, and $Mg^{2+}$. Oxyluciferin is formed as a reaction product in an electronically excited state, emitting light on transition to the ground state.

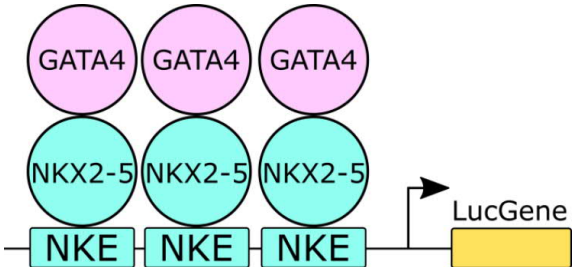


**Figure 5** Luciferase assay setup for synergistic activation of the reporter gene containing three NKX-binding sites (NKE). The assay can detect either inhibitors or enhancers of synergistic activation. Adapted from Publication II.

## 2.2 [3+2] DIPOLAR CYCLOADDITION REACTIONS FOR SYNTHESIS OF THE ISOXAZOLE CORE

Synthesis of isoxazole-based compounds has drawn much interest during the last decades since isoxazoles show activity in multiple different targets such as enzyme cyclooxygenase 2 (COX-2),[40] growth hormone secretagogue receptor (GHS-R),[41] human dihydroorotate dehydrogenase (DHODH),[42,43] and bromodomain-containing protein 4 (BRD4).[44] Molecular structures (**4**–**8**) with the aforementioned biological targets are presented in **Figure 6**. Isoxazole synthesis is well established and in recent years there have been remarkable advances in the cycloaddition, cycloisomerization, condensation, and direct functionalization methods.[45] The [3+2] dipolar cycloaddition reaction has a long history dating back to the 1930s, when Quilico[46,47] reported the first isoxazole forming reactions between nitrile oxides and alkynes. To date, [3+2] dipolar cycloaddition reaction is still considered the most important method for the synthesis of isoxazoles.[45]

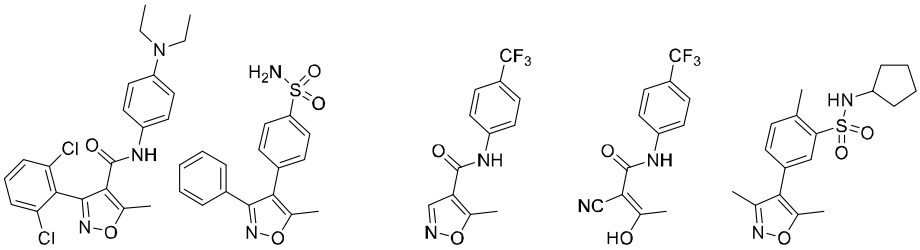


**Figure 6** Molecular structures of isoxazole compounds targeting various biological pathways. Compound **7** (A771726) is an active metabolite of leflunomide.

### 2.2.1 REACTION MECHANISM AND REGIOCHEMISTRY

The reaction mechanism of [3+2] dipolar cycloaddition has been intensively studied, as there are usually at least two possible regioisomers formed in the reaction. Previously, poor regioselectivity has limited its use for broad range of substrates but recent advances in metal-catalyzed reactions have helped to overcome the challenge.[45]

Regiochemical prediction in [3+2] dipolar cycloaddition reactions is based on Fukui's frontier molecular orbital (FMO) theory[48], which states that interacting molecular orbitals (MO) are most stabilized when their energy difference is smallest. Sustmann and Trill[49] successfully applied FMO to [3+2] dipolar cycloaddition reactions and explained the earlier findings of Huisgen[50], i.e. the reactivity of [3+2] dipolar cycloaddition reaction of phenyl azide is increased both by electron-attracting and by electron-donating substituents. They discovered that the substituent effect is context dependent, i.e. it depends on the highest occupied molecular orbital (HOMO) and lowest unoccupied molecular orbital (LUMO) differences of the dipolarophile and dipole. There are three different possibilities based on the relative positions of frontier orbitals (**Figure 7**): (1) $HOMO_{dipolarophile}$-$LUMO_{dipole}$ interaction is dominant; (2) both interactions need to be taken into account and interaction in which energy is reduced more due to the substituent becomes a decisive factor for reactivity; or (3) $LUMO_{dipolarophile}$-$HOMO_{dipole}$ is dominant.

Accordingly, substituents that increase the dipole HOMO energy or decrease dipolarophile LUMO energy will accelerate type 1 reactions.[51] Furthermore, substituents that decrease the dipole LUMO energy or increase dipolarophile HOMO energy will accelerate type 3 reactions.[51] Type 2 reactions are accelerated in both of the aforementioned ways.[51]

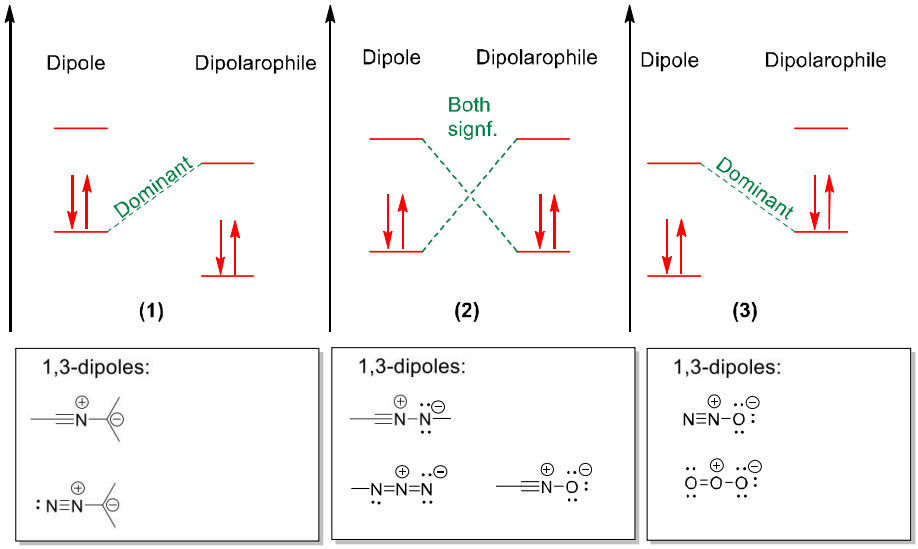


**Figure 7** Three options for frontier orbitals that determine the dominant energy difference for the substituent effect in [3+2] dipolar cycloaddition. Examples of 1,3-dipoles for each reaction type.[52]

Isoxazoles are generally made of a nitrile oxide acting as the 1,3-dipole and an alkyne as the dipolarophile. Regiochemistry of the reaction is determined based on HOMO and LUMO interactions of the 1,3-dipole and dipolarophile.[53,54] Two possible outcomes are described in **Figure 8**.

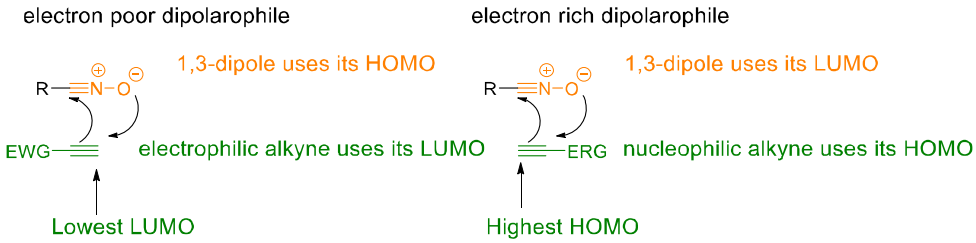


**Figure 8** Two alternative reactions determining regiochemistry of the [3+2] cycloaddition reaction between nitrile oxide and either electrophilic or nucleophilic alkyne. Abbreviations: EWG, electron withdrawing group, ERG, electron releasing group.

### 2.2.2 REACTIONS AND SYNTHESIS

The nitrile oxide-mediated synthesis of isoxazoles has recently gained great interest, as nitrile oxides can be generated *in situ* from oximes by using different oxidizing agents such as hypervalent iodine reagents and Oxone®, i.e. the triple salt $2KHSO_5 \cdot KHSO_4 \cdot K_2SO_4$.[55–57] Previously, nitrile oxides were generated from oxime halides in basic conditions,[58,59] until recent publication by Kesornpun et al., which showed that the reaction also works in acidic

conditions (pH 4) and in water.[60] Two different routes for nitrile oxides are presented in **Figure 9**. In addition, isoxazoles have been prepared via different catalytic methods using transition metals, such as ruthenium or palladium[61,62] and copper[63] as catalysts. Metal catalyst can remarkably increase selectivity in a [3+2] dipolar cycloaddition.[63]

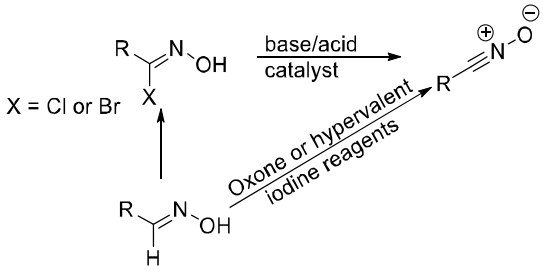


**Figure 9** Different synthetic routes to prepare nitrile oxides.

## 2.3 TOXICITY MECHANISMS OF DIFFERENT RING SYSTEMS

Understanding the chemical reactivity and metabolism of different ring systems is extremely important in drug discovery. For example, a phenyl ring is the most prevalent ring system in drug molecules.[64,65] Generally, phenyl-ring systems in drugs are safe, but their metabolism has been extensively researched as their toxicity is mainly mediated by reactive metabolites.[66] Moreover, there are some reports of DNA intercalation of the relatively flat, multiple fused aromatic-ring–containing compounds.[67] Furthermore, furan rings are rarely seen in drug candidates as they are easily metabolized to various electrophilic products further reacting with proteins or DNA and causing toxicity.

### 2.3.1 CYTOCHROME P450 METABOLISM

Oxidative metabolism of phenyl rings mediated by the cytochrome P450 (CYP) enzyme family is of great interest from the drug discovery point of view.[68] Oxidative metabolism of arenes by CYP enzymes is important as it has been linked to the formation of covalently binding metabolites.[66] Two different routes for acid-catalyzed oxidative metabolism of a phenyl ring are presented in **Figure 10**. The direct pathway involves the loss of metabolically labile hydrogen, while in the indirect pathway the hydrogen migrates to the α-carbon.

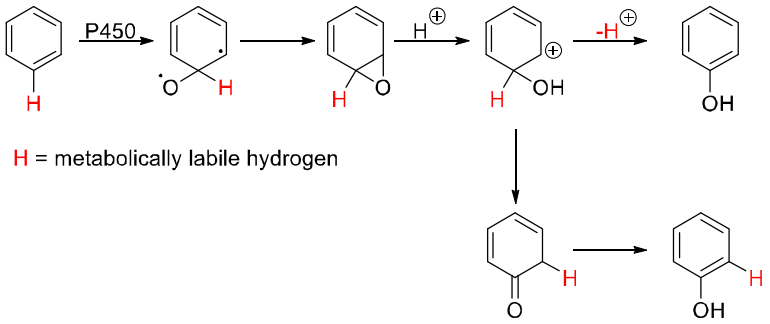


**Figure 10** P450-catalyzed epoxidation of phenyl rings.

P450 enzymes also catalyze oxidation of heterocycles such as furan rings to reactive metabolites.[69] Trapping reactions with glutathione (GSH) have shown that furan oxidation can proceed via either *cis*-enedione or direct addition to the carbon adjacent to furanyl oxygen.[69] P450 enzyme-mediated oxidation of furan to either epoxide or *cis*-enedione and their subsequent reactions with GSH are presented in **Figure 11**.

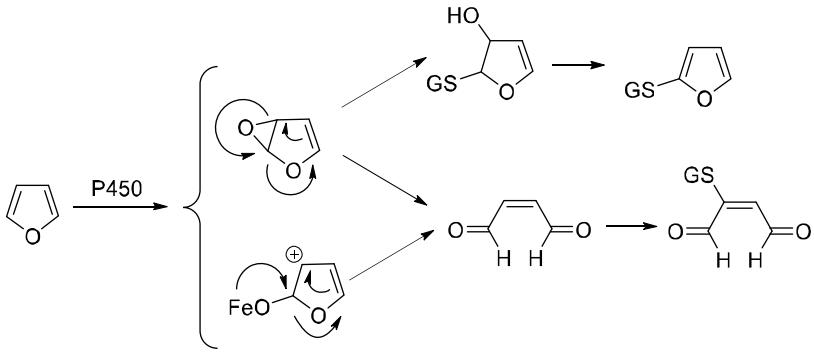


**Figure 11** P450-catalyzed oxidation of furan to either epoxide or *cis*-enedione and subsequent reaction with GSH.[70,71]

The computational prediction of oxidative reactions that potentially generate toxic metabolites to identify labile sites of metabolism is intriguing, as a vast majority of the drugs containing phenyl rings, for instance, are safe.[66,68] Computational methods are generally based on density functional theory (DFT) calculations and ligand docking to the various CYP enzyme isoforms.[68] DFT calculations predict the accurate activation energies needed for the oxidation reaction for each site on the substrate.[72]

### 2.3.2 STACKING INTERACTIONS OF RINGS IN DRUGS

Stacking interactions play a pivotal role in biological systems.[73] These interactions can be considered to be a major driving force for the binding of potentially cytotoxic DNA intercalators.[74] Generally, stacking interactions mean face-to-face interactions of approximately parallel and planar π-systems (**Figure 12a**).[75] From the structure-based drug design point of view, the stacking interactions to aromatic amino acid side chains (Phe, Tyr and Trp, see **Figure 12b**) are especially interesting. [76] One recent example of such interactions can be found between the Phe residue of human cystic fibrosis transmembrane conductance regulator and oxoquinoline part of ivacaftor (**Figure 13**).[77]

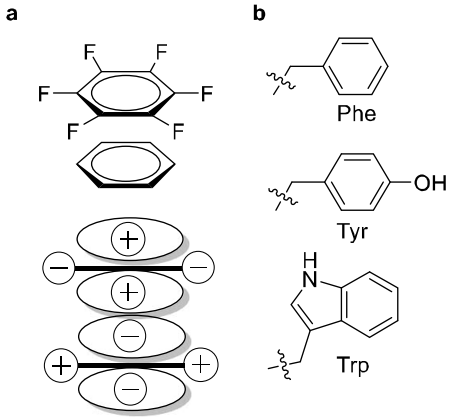


**Figure 12** (a) Face-to-face stacking interaction;[73] (b) aromatic amino-acid side-chains.

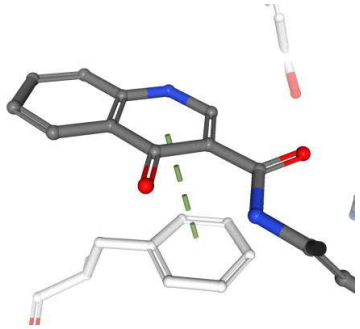

**Figure 13** Stacking interaction of oxoquinoline and the Phe residue in human cystic fibrosis transmembrane regulator; image created with NGL Viewer[78] (PDB 602P).

Calculating stacking interaction energies is computationally heavy as it requires the use of quantum mechanical methods and systematic exploration to determine the global minimum energy of the stacked structure.[76] However, a recent study of Bootsma and Wheeler[76] showed that stacking interaction

energies can be predicted accurately based on simple electrostatic potential descriptors of rings with no quantum chemical calculations.

### 2.3.3 DNA INTERCALATION

Planar π-systems have been also associated with drug intercalation to DNA.[79,80] π-Interactions are regarded as the major driving force for intercalator binding.[74] Proflavine is an example of a classic DNA intercalator, that binds between adjancent DNA bases (**Figure 14**).[81] More sequence specificity can be obtained with threading intercalators, which extend their binding to either a minor or major groove.[82]

DNA intercalation is a very interesting topic in drug design as it has been associated with cytotoxicity[80] of some drugs and it could be exploited[83] when designing new inhibitors of transcription factors.

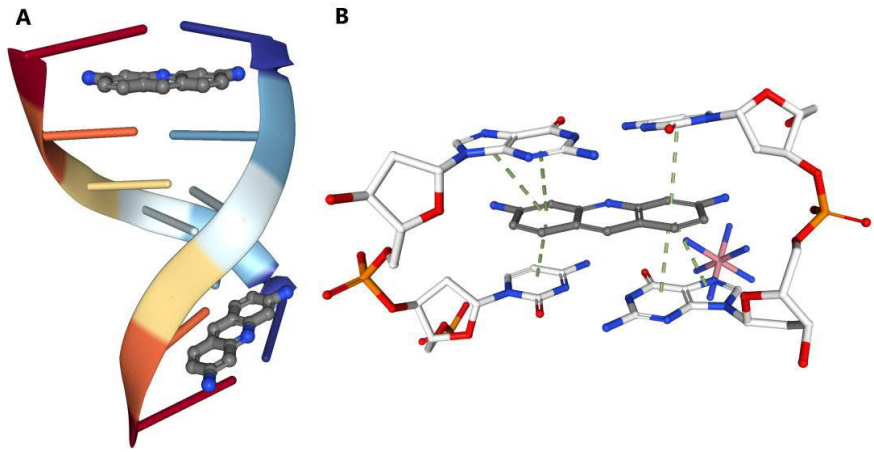


**Figure 14** (a) Proflavine intercalating to DNA; (b) π-interactions (green lines) of aromatic DNA bases and proflavine; images created with NGL Viewer[78] (PDB 3FT6).

## 2.4 TARGET IDENTIFICATION WITH AFFINITY CHROMATOGRAPHY

Target identification is a crucial step for projects focused on phenotypic drug discovery.[84] Affinity chromatography is a method used for determining the protein targets of small molecular compounds by either immobilizing a compound to a solid phase or by tagging a compound with a fluorescent group, for example.[85] Affinity chromatography has been successfully used to identify

targets of bioactive compounds and drugs in clinical use, such as diminutol,[86] imatinib,[87] purvalanol,[88] roscovitine,[89] thalidomide,[90] and vancomycin.[91] In affinity chromatography, the compound of interest is attached to a solid phase, such as Sepharose® with a linker molecule.[85] Generally, linker molecules are based on either alkyl chains or preferably polyethyleneglycol (PEG). Hydrophilic PEG linkers usually decrease the amount of non-specific binding to the proteins compared to hydrophobic alkyl linkers.[92] Different types of linkers are described in **Figure 15**. The immobilized compounds are incubated with protein lysate and the unbound proteins are washed away in several steps followed by identification of the bound proteins, either with sodium dodecyl sulfate polyacrylamide gel electrophoresis (SDS-PAGE) or tryptic digestion and identification of the resulting peptides by MS/MS mass spectrometric analysis (**Figure 16**).[92]

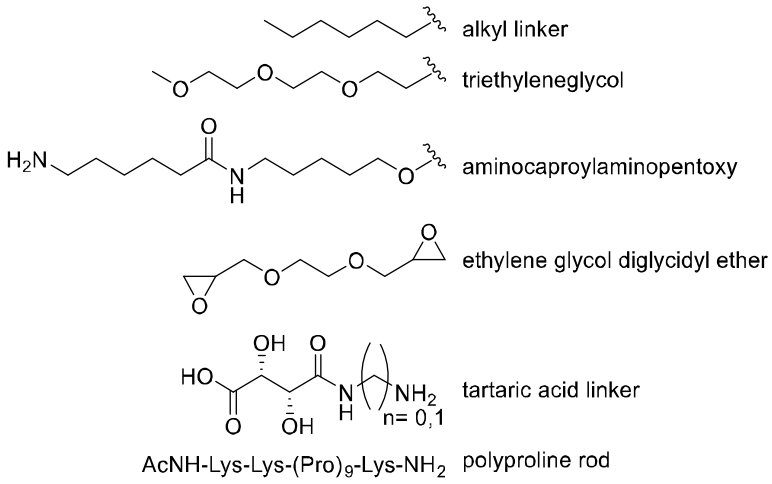


**Figure 15** Various linkers for affinity chromatography.[92]

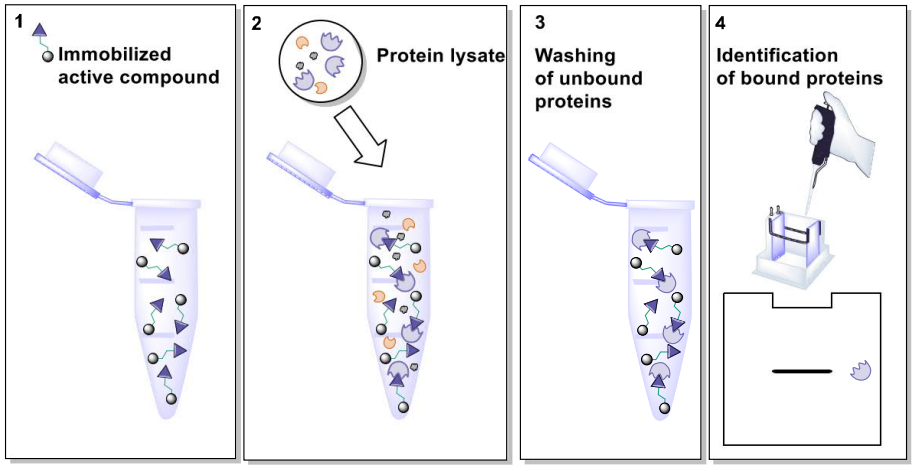


**Figure 16** Schematic presentation of affinity chromatography. Modified from Publication III.

Performing a successful affinity chromatography experiment requires deep understanding of the SAR of the compound of interest.[93] This is crucial because a linker compound has to be attached in a way that compound binding to the target is not extensively affected. Attaching the linker to the active compound is not always straightforward, because suitable functional groups may be lacking in the compound of interest or synthethic challenges may pose problems in cases of more complex molecules.[93]

It is difficult to avoid non-specific binding completely, but amount of it can be approximated by using a negative control.[93] Negative controls are used to distinguish specific targets from background binding.[93] A simplest negative control is the matrix without a ligand, although the matrix linked to the non-binding ligand is considered a better option.[93] This strategy was succesfully applied by Oda et al.[94] in their study where they identified the primary target of the anticancer agent E7070. The matrix-immobilized E7070 and its negative amide control are shown in **Figure 17**.

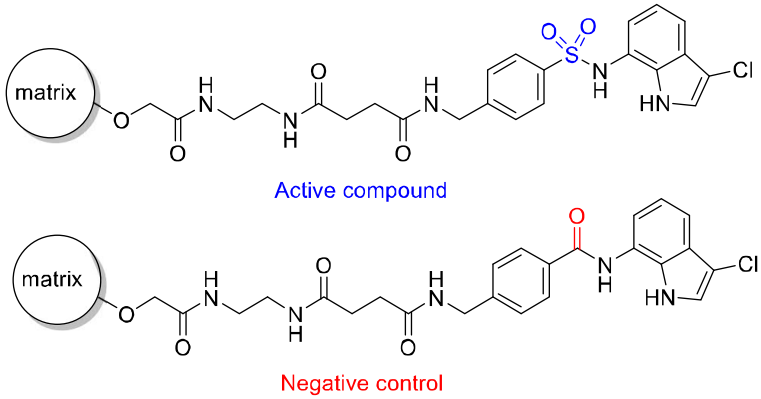


**Figure 17** Immobilized E7070 and its negative amide control.

# 3 AIMS OF THE STUDY

The general aims of the study were to design and synthesize nontoxic GATA4-NKX2-5 interaction inhibitors with antihypertrophic activity and determine their mechanism of action.

The more specific aims were:

- Design and synthesis of isoxazole derivatives and exploration of different cycloaddition methods (I) & (II)
- Analysis of luciferase assay and cytotoxicity data to select compounds for further evaluation (II)
- Validation of the mechanism of action of the hit compound with affinity chromatography (III)

# 4 RESULTS AND DISCUSSION

## 4.1 SYNTHESIS OF 3,4,5-TRISUBSTITUTED ISOXAZOLE DERIVATIVES (PUBLICATIONS I & II)

To study different heterocyclic rings as a replacement for the hit compound's (**1**) phenyl ring at the 3-position of an isoxazole ring, we designed various bis-heterocycles (**5a-e**). In addition, one pyrazole derivative (**5f**) was synthesized with a similar method. The synthesis procedure is presented in **Scheme 1**. Compounds **5a-f** were synthesized starting from the commercially available aldehydes (**1a-e**), which were converted to the corresponding oximes (**2a-g**) in the presence of hydroxylamine hydrochloride. The oximes were used to generate nitrile oxide intermediates for 1,3-dipolar cycloadditions in the presence of various oxidants: diacetoxyiodobenzene (DIB), Oxone®, or [hydroxy(tosyloxy)iodo)] benzene (HTIB). Various methods to synthesize isoxazole esters **3a-g** from ethyl 2-butynoate and oximes **2a-g** are listed in more detail in **Table 2**. Generally, a lower dipole moment containing oximes with thiophene (**2c** or **2e**) or phenyl (**2f**) rings seemed to work better compared to the higher dipole moment containing oximes with furan (**2b**), oxazole (**2a**), or isoxazole (**2d**) rings. A lower dipole moment of the reactant could increase reaction rate in a polar solvent as the transition state does not involve charge separation and the reaction itself is not dependent on solvent polarity.[95] However, it is difficult to draw firm conclusions as different methods were used to generate reactive nitrile oxides. Interestingly, water could be used as a solvent for dipolar cycloadditions.[96] It has been shown previously that water increases the rate of the 1,3-dipolar cycloadditions when compared to organic solvents.[97] Furthermore, isoxazole esters **3a-g** were hydrolyzed to carboxylic acids **4a-g** with NaOH in an equimixture of $H_2O$ and MeOH. Carboxylic acids **4a-g** were further coupled with *N,N*-diethyl-*p*-phenylenediamine in the presence of *N,N,N′,N′*-tetramethyl-*O*-(1*H*-benzotriazol-1-yl)uronium hexafluorophosphate (HBTU) and *N,N*-diisopropylethylamine (DIPEA).

**Table 2** Reaction conditions for 1,3-dipolar cycloaddition reactions.

| Cmpd | Oxidant | Catalyst | Solvent | Yield |
|---|---|---|---|---|
| **3a** | HTIB | - | $H_2O$ | 20% |
| **3b** | DIB | TFA | MeOH | 19% |
| **3c** | DIB | TFA | MeOH | 32% |
| **3d** | Oxone | PhI | $H_2O$ | 7% |
| **3e** | Oxone | KCl | $H_2O$ | 42% |
| **3f** | Oxone | KCl | $H_2O$ | 55% |

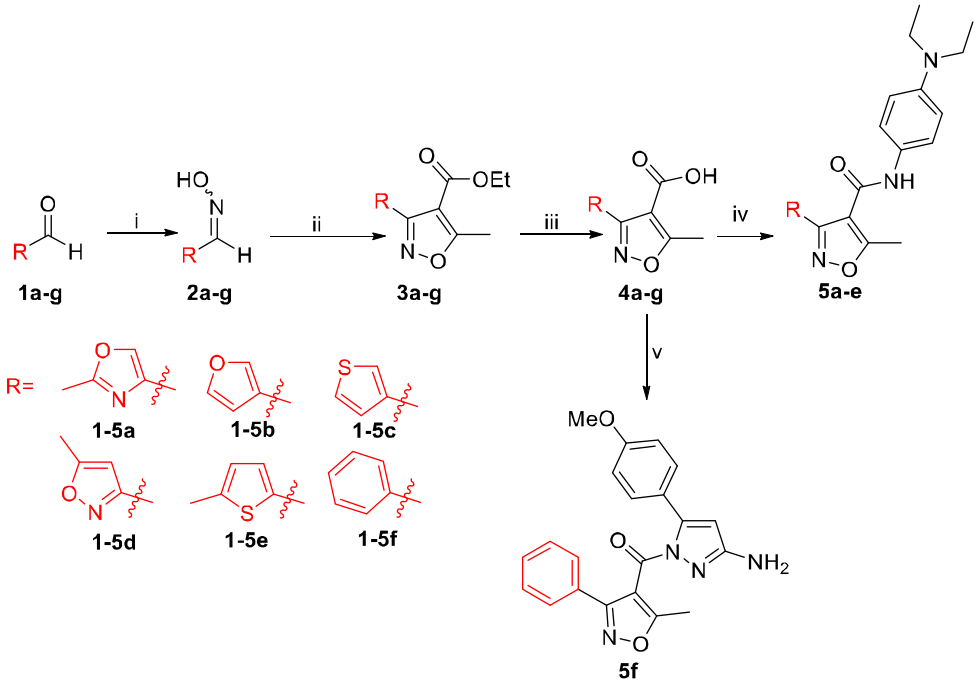


**Scheme 1** Synthesis of bis-heterocycles and pyrazole. Reagents and conditions: (i) **2a**: $H_2NOH$-HCl, NaOAc, MeOH, rt, **2b-f**: $H_2NOH$-HCl, pyridine, EtOH, rt; (ii) **3a**: ethyl but-2-ynoate, HTIB, $H_2O$, rt, 2 h, **3b-c**: ethyl but-2-ynoate, DIB, trifluoroacetic acid (TFA), MeOH, 0 °C→rt, 2−3 h, **3d**: ethyl but-2-ynoate, Oxone®, PhI, $H_2O$, rt, 18 h, **3e-f**: ethyl but-2-ynoate, Oxone®, KCl, $H_2O$, rt, 4-5 h; (iii) **4a-f** $H_2O$/MeOH (1:1), NaOH, 60 °C (or rt for **4d**), 1 d; (iv) *N*,*N*-diethyl-*p*-phenylenediamine, HBTU, DIPEA, *N*,*N*-dimethyl formamide (DMF), rt, 1−2 d; (v) 3-amino-5-(4-methoxyphenyl)pyrazole, HBTU, DIPEA, DMF, rt, 18 h.

## 4.2 SCAFFOLD HOPPING (PUBLICATION II)

To test whether a phenyl ring in the northern part of compound **1** could be replaced with a heterocycle, we synthesized a thiazole derivative **8** (**Scheme 2**). Compound **8** was synthesized from 1-bromopinacolone **6**, which was reacted with thiourea in ethanol under microwave irradiation at 120 °C to get 4-(*tert*-butyl)thiazol-2-amine **7**. Thiazolamine **7** was further coupled with 5-methyl-3-phenylisoxazole-4-carboxylic acid in the presence of HBTU and DIPEA.

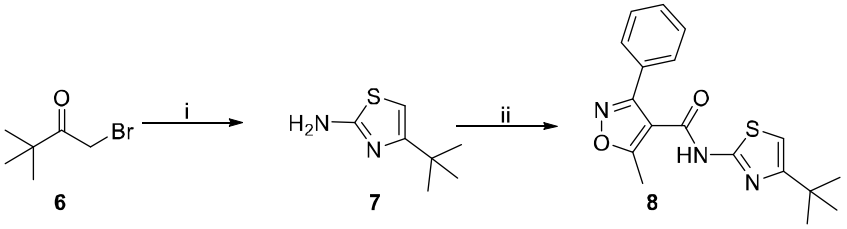


**Scheme 2** Synthesis of thiazole derivative **8**. Reagents and conditions: i) EtOH, mw (100 °C, 30 min); ii) 5-methyl-3-phenylisoxazole-4-carboxylic acid, HBTU, DIPEA, DMF, rt, 1 d.

Based on the preliminary data, we had a reason to believe the bisisoxazole core to be a potentially optimal scaffold for biological activity. We decided to study bisisoxazole scaffold further by synthesizing derivatives where we either kept bisisoxazole core intact or explored different heterocycles in the place of the isoxazole attached to the central part of the molecule (**Scheme 3**). Carboxylic acids were acquired from Enamine Ltd and coupled with *N,N*-diethyl-*p*-phenylenediamine in the presence of HBTU and Hünig's base in DMF at room temperature. Yields varied between 63% and 88%. The small scale of synthesis created some purification problems that were overcome by triturating the crude product with either *n*-heptane or diethyl ether. None of the synthesized compounds were notably active in the GATA4-NKX2-5 transcriptional synergy assay, indicating that the isoxazole ring is not the best replacement for the hit compound's phenyl ring in the southern part.

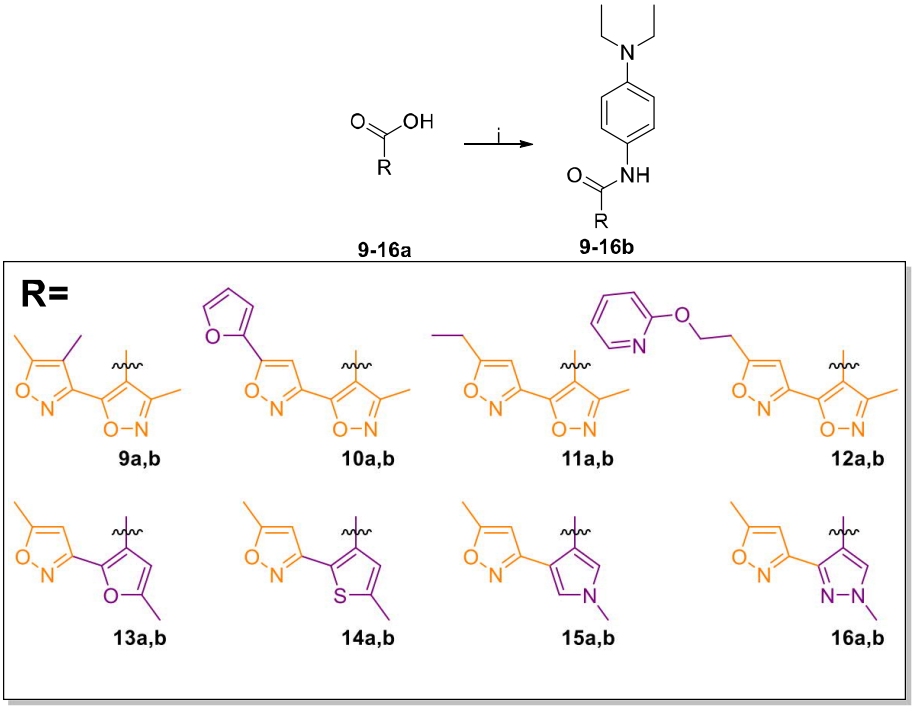


**Scheme 3** Amide coupling reaction to get different heterocyclic scaffolds. Reagents and conditions: (i) *N,N*-diethyl-*p*-phenylenediamine, HBTU, DIPEA, DMF, rt, 1 d.

## 4.3 SAR ANALYSIS (PUBLICATION II)

The original hit compound **1** was divided into three parts (southern, northern and central part) based on the structural modifications carried out (**Figure 18**). In the southern part of the compound, different heterocycles were tested as a surrogate of the phenyl ring. In addition, different scaffolds were tested in place of the isoxazole core ring structure. In the central part of the compound, the central amide group was replaced with alkyl, thioamide, inverse amide, imino and ether linkers. In the northern part of the compound, mainly *para* substitution of the compound was studied.

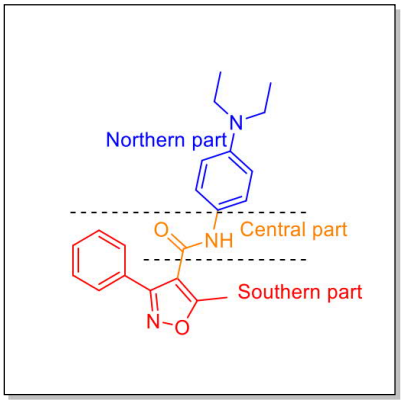


**Figure 18** Hit compound **1** and its subsections.

### 4.3.1 SOUTHERN PART

To identify structural features affecting the inhibition of GATA4-NKX2-5 transcriptional synergy, we first explored the chemical space around the southern part of the original hit compound **1**. Different scaffolds for the southern part of the compound were either synthesized in-house or acquired commercially. The most interesting activity cliffs of the molecular pairs in the scaffold hopping endeavor are presented in **Table 3**. Interestingly, reversing a substitution pattern from compound **1** to **65** increased activity by approximately 20% in the GATA4-NKX2-5 synergy assay. A similar trend can be seen with compounds **390** and **3**. In this case, activity of the inactive compound **390** increases by approximately 20% in the reversely substituted isoxazole (**3**). This indicates that the isoxazole core plays an important role in activity of the compounds. In addition, inhibition of transcriptional synergy decreases approximately 50% when the phenyl ring of the compound **65** is replaced with the isoxazole ring in compound **3**. Furthermore, 5-phenylisoxazole (**47d**) without a methyl substituent is inhibiting approximately 20% less GATA4-NKX2-5 transcriptional synergy than the 3-methyl-5-phenylisoxazole (**65**) counterpart. Surprisingly, replacing the phenyl ring of compound **47d** with a cyclopropyl ring (**47r**) converts the compound to an enhancer of the transcriptional synergy of GATA4 and NKX2-5. In a series of pyrazole compounds, the phenyl ring (**47e**) seems to work again better than isoxazole (**47f**) as a ring replacement. A similar observation can be made concerning synergy inhibition of 5-methyl-2-phenylfuran (**54**) when compared to 3-(5-methylfuran-2-yl)-5-methylisoxazole (**47h**). Interestingly, changing one nitrogen to sulfur (**47n**) in the phenyltriazole (**47o**) decreases transcriptional activity from 84% to 41% of control. A drastic change in transcriptional synergy inhibition, approximately 80%, can also be seen in a plain thiophene (**55**) when compared to isothiazole (**47s**), 2-nitrothiophene (**47u**), or 2-methyl-3-phenylthiophene (**47t**). Activity

of 2-methyl-3-phenylthiophene (**47t**) is lost if its phenyl ring is replaced with a pyrrole ring as in compound **56**. Finally, the fused ring systems (**47v** and **47aa**) might be good scaffolds for transcriptional synergy enhancers. Synergy enhancing activity of the compound **47aa** is lost with a removal of one nitrogen and and addition of a methyl substituent in a compound **47ab**.

**Table 3** Representative examples of scaffold hopping of the southern part of the compound **1** and their transcriptional synergy inhibition (% of control) at 10 µM concentration. Compound numbers are from Publication II.

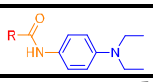

| Cmpd | R | Synergy (% of control) Mean ± SD | Cmpd | R | Synergy (% of control) Mean ± SD |
|---|---|---|---|---|---|
| **1** | 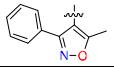 | 50 ± 9.5 | **65** | 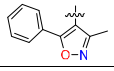 | 29 ± 5.0 |
| **390** | 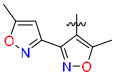 | 100 ± 13 | **3** | 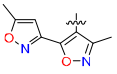 | 78 ± 13 |
| **47r** | | 140 ± 4.3 | **47d** | 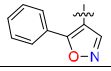 | 47 ± 9.8 |
| **47f** | | 99 ± 11 | **47e** | 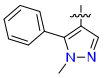 | 62 ± 1.5 |
| **47h** | 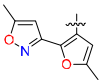 | 100 ± 6.1 | **54** | 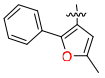 | 35 ± 2.9 |
| **47o** | 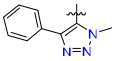 | 84 ± 4.5 | **47n** | 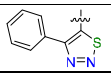 | 41 ± 2.2 |
| **55** | | 110 ± 32 | **47s** | | 27 ± 12 |
| **56** | 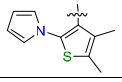 | 79 ± 12 | **47t** | 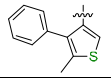 | 33 ± 6.2 |
| **47v** | | 130 ± 14 | **47u** | | 25 ± 6.3 |
| **47aa** | | 140 ± 2.7 | **47ab** | 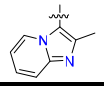 | 78 ± 17 |

As it seemed evident that the isoxazole substituent regulates compound activity, the substituent effect was researched in more detail with different heterocycles and phenyl rings (**Table 4**). First, the effect of different substituents in the phenyl ring of the hit compound was considered. We noticed that an electron withdrawing substituent (Br and $NO_2$) in the *para* position of the phenyl ring (compounds **39i** and **39a**) remarkably reduced the synergy inhibition. The *meta* position (**39g**) was the optimal position for the nitro group, which still led to 15% lower synergy inhibition. Interestingly, *ortho*-dichloro substitution (**39f**) did not affect synergy inhibition of the *meta*-substituted nitrophenyl. However, the removal of the nitro group led to diminished synergy inhibition in *ortho*-dichloro and monochloro-substituted compounds (**39e** and **39k**). In pyridine rings, "*ortho*" nitrogen (**59**) diminished synergy inhibition while "*para*" nitrogen (**39c**) did not affect synergy inhibition remarkably (50% compared to 61%). These data indicate that the activity of the compounds is not dominated by the electronic effect of the ring. The most potent synergy inhibitor in this series was a *para* fluorine-substituted compound **39d**. Interestingly, it also inhibited less GATA4 transcriptional activity (79%) than the original hit compound **1** (62%) at 10 μM concentration. It is unlikely that electronegativity of the fluorine atom is the main contributor to the increased synergy inhibition as other electron withdrawing substituents in the same position did not increase synergy inhibition. One possible explanation could be a direct contribution to the binding affinity through either hydrogen bond or hydrophobic interactions.[98] Activity is lost with the addition of an extra phenyl ring in compound **39j** indicating that there is a limited space in that region of the binding pocket. Of the tested five-membered heterocycles, only 3-thiophene **39m** showed noticeable inhibition of the transcriptional synergy of GATA4 and NKX2-5. The plain alkyl chain led also to the diminished inhibition of transcriptional synergy in compound **39b**.

**Table 4** Isoxazoles substituted with various heterocycles and phenyl rings and their transcriptional synergy inhibition (% of control) at 10 µM concentration. Compound numbers are from Publication II.

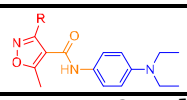

| Cmpd | R | Synergy (% of control) Mean ± SD | Cmpd | R | Synergy (% of control) Mean ± SD |
|---|---|---|---|---|---|
| **39i** | | 70 ± 6.4 | **1** | | 50 ± 9.5 |
| **39a** | 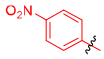 | 100 ± 16 | **39g** | 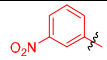 | 65 ± 3.7 |
| **39h** | | 84 ± 1.3 | **39f** | 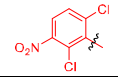 | 66 ± 2.6 |
| **39e** | | 110 ± 5.0 | **39k** | | 88 ± 14 |
| **59** | | 100 ± 0.41 | **39c** | | 61 ± 7.5 |
| **39j** | 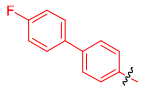 | 110 ± 12 | **39d** | | 44 ± 1.1 |
| **39p** | | 100 ± 2.0 | **39l** | | 89 ± 25 |
| **39n** | | 110 ± 5.8 | **39m** | | 66 ± 4.2 |
| **39b** | | 100 ± 0.85 | **60** | | 100 ± 6.1 |

### 4.3.2 CENTRAL PART

Next, the search continued for an optimal central part of the compounds inhibiting transcriptional synergy of GATA4 and NKX2-5 (**Table 5**). Interestingly, activity of the original hit compound **1** was completely lost with methylation of the amide bond in compound **25a**. However, bigger benzyl (**25c**) and fluoroethyl (**25b**) substituents were tolerated, which was particulary important regarding the target validation study (Publication III). The reversed amide bond (**27**) and sulfonamide (**21**) linker led to the diminished synergy inhibition. Interestingly, the most potent inhibitors of the transcriptional synergy of GATA4 and NKX2-5 were N-acylated amines **58** and **30c**. As imines (**19** and **31**) or amines (**20** and **33**) were not promising replacements for the amide bond, one could conclude that a hydrogen bond acceptor is a required feature in the central part. This observation was further

validated, because thioamide as a weaker hydrogen bond acceptor was not a suitable replacement for an amide in compounds **23** and **26**.

**Table 5** Different central parts for inhibition of transcriptional synergy between GATA4 and NKX2-5 (% of control) at 10 µM concentration. Compound numbers are from Publication II.

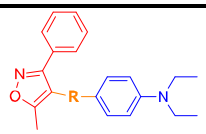

| Cmpd | R | Synergy (% of control) Mean ± SD | Cmpd | R | Synergy (% of control) Mean ± SD |
|---|---|---|---|---|---|
| **1** | | 50 ± 9.5 | **25a** | | 97 ± 9.9 |
| **25c** | 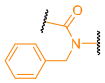 | 66 ± 13 | **25b** | | 79 ± 0.092 |
| **27** | | 94 ± 14 | **21** | | 98 ± 16 |
| **16** | | 80 ± 23 | **58** | | 22 ± 4.9 |
| **19** | | 100 ± 2.6 | **31** | | 96 ± 12 |
| **20** | | 100 ± 3.7 | **33** | | 91 ± 20 |
| **23** | | 99 ± 7.8 | **30a** | | 82 ± 8.0 |
| **26** | | 91 ± 3.5 | **30c** | 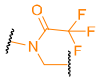 | 52 ± 23 |

### 4.3.3 NORTHERN PART

Finally, different northern parts with amide or ether linkers were tested (**Table 6**). Surprisingly, the compound with a dimethylaniline-substituted northern part (**4d**) was completely inactive, indicating the existence of the important hydrophobic interaction. Indeed, this hypothesis is reinforced with the observed inhibitory activity of the branched alkyl group (**4i**) and bulky 4-chromen-4-one (**4g**) derivatives. Methylation of *N*-ethyl-*N*-isopropylaniline **4i** led to a decreased inhibitory effect on transcriptional synergy in compound **7**. Activity decreased in a similar manner if either an electron withdrawing nitro group (**8**) or an electron donating amino group (**9**) were added to the

northern part phenyl ring. This indicates that the acid strength of aniline is not important for the compound activity. Interestingly, the diethylaniline group of the original hit compound **1** could be replaced with an ethynyltrimethylsilane group (4**j**) and retain a weak inhibitory effect. The replacement of the phenyl ring with a thiazole in compound **4k** completely abolished the inhibition of the transcriptional synergy of GATA4 and NKX2-5. In addition, a carboxylic acid **12** and carbocylic acid esters with nitrile groups **10a-c** were tested, but none showed any significant activity in the GATA4-NKX2-5 transcriptional synergy assay.

However, nitriles with ether-type central-part linkers, **35a** and **35b,** inhibited transcriptional synergy potently (26% and 52% of control, respectively). (1-Methoxypropyl)phenyl substitution in **34e** also showed similar activity (43% of control) as the original diethylaniline northern part in compound **1** (50% of control). Interestingly, the polar ester derivative with an oxopropyl group (**35d**) also showed a promising inhibitory effect (37% of control). Neither of the alkyl derivatives (**34c** and **35e**) or amides (**36a** and **36b**) showed any activity.

**Table 6** Various northern parts with amide and ether linkers and their transcriptional synergy inhibition (% of control) at 10 µM concentration. Compound numbers are from Publication II.

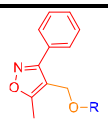

| Cmpd | R | Synergy (% of control) Mean ± SD | Cmpd | R | Synergy (% of control) Mean ± SD |
|---|---|---|---|---|---|
| **4d** | 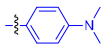 | 99 ± 8.6 | **34a** | 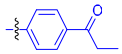 | 76 ± 18 |
| **4g** | 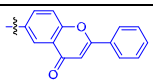 | 31 ± 7.5 | **34b** | 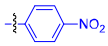 | 85 ± 3.9 |
| **4i** | 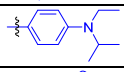 | 41 ± 1.5 | **34c** | 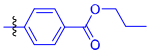 | 110 ± 9.7 |
| **7** | 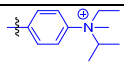 | 83 ± 9.5 | **35e** | 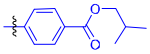 | 99 ± 22 |
| **8** | 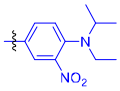 | 75 ± 4.2 | **36a** | 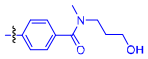 | 100 ± 9.7 |
| **9** | 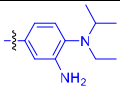 | 76 ± 3.4 | **36b** | 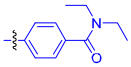 | 92 ± 18 |
| **4j** | 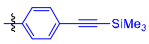 | 69 ± 5.5 | **34d** | 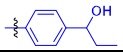 | 87 ± 20 |
| **4k** | 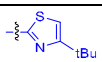 | 110 ± 14 | **34e** | 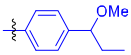 | 43 ± 3.5 |
| **10a** | 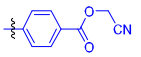 | 90 ± 6.2 | **35a** | 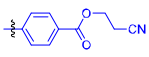 | 26 ± 0.42 |
| **10b** | 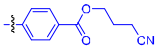 | 98 ± 3.5 | **35b** | 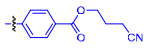 | 52 ± 8.3 |
| **10c** | 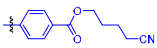 | 90 ± 3.3 | **35c** | 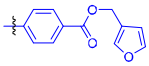 | 100 ± 8.7 |
| **12** | 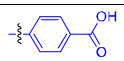 | 98 ± 11 | **38** | 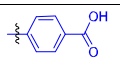 | 120 ± 5.3 |
| **11** | 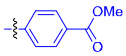 | 92 ± 3.3 | **35d** | 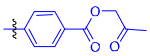 | 37 ± 3.0 |

## 4.4 CYTOTOXICITY (PUBLICATION II)

To determine whether a compound toxicity potentially influenced the observed activities in luciferase assays, 40 compounds were selected for toxicity testing in the lactate dehydrogenase (LDH) and 3-(4,5-dimethylthiazol-2-yl)-2,5-diphenyltetrazolium (MTT) bromide assays (**Figure 19**). None of the compounds induced any significant necrosis to COS-1 cells in an LDH assay. The most toxic compounds for COS-1 cells in the MTT assay are displayed in **Table 7**. Interestingly, ether (**34a**, **34e,** and **34d**) and N-acylated amine (**30c**, **58,** and **64**) central-part–containing compounds seemed to be more toxic than the amides.

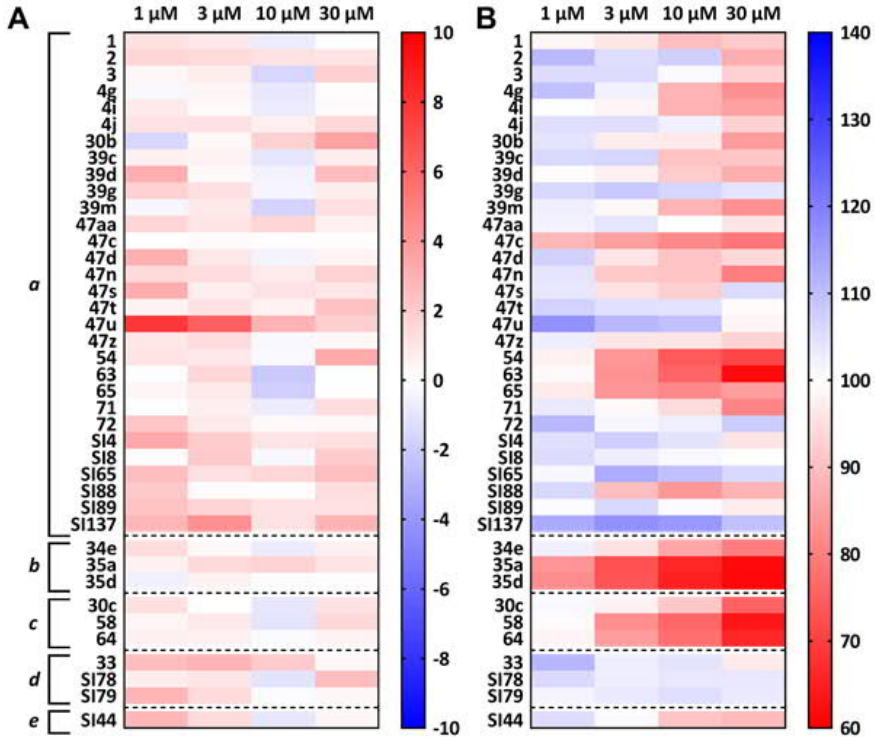


**Figure 19** Cytotoxicity of the compounds to COS-1 cell line. A; Compound-induced necrosis in an LDH assay after 24 h exposure (% of maximal LDH release). B; Cell viability in the MTT assay after 24 h compound exposure. The data represent means from 2–3 independent experiments and are presented as % of control. Grouping is based on the central part of the compounds: *a*, amide; *b*, ether; *c*, N-acylated amine; *d*, amine and *e*, imine. Compound numbers are from Publication II.

**Table 7** Most toxic compounds in an MTT assay (COS-1; 3 µM and 10 µM concentrations; the cell viability data are presented as % of control). Compound numbers are from Publication II.

| Cmpd | Structure | 3 µM | 10 µM |
|---|---|---|---|
| **35d** | 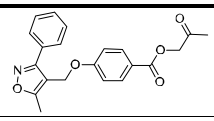 | 73 ± 19 | 65 ± 19 |
| **35a** | 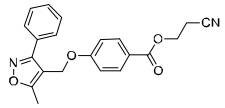 | 73 ± 5.1 | 66 ± 7.3 |
| **54** | 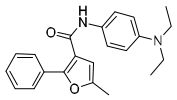 | 84 ± 11 | 74 ± 13 |
| **63** | 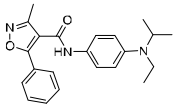 | 83 ± 7.1 | 76 ± 3.8 |
| **58** | 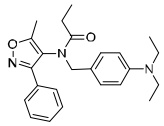 | 82 ± 6.5 | 76 ± 4.3 |
| **64** | 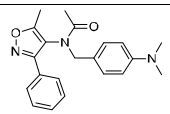 | 85 ± 6.2 | 77 ± 4.6 |
| **65** | 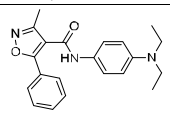 | 83 ± 2.1 | 81 ± 1.6 |
| **47c** | 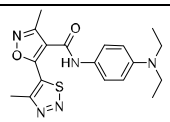 | 85 ± 5.0 | 82 ± 0.9 |
| **SI88** | 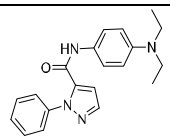 | 90 ± 1.1 | 84 ± 1.1 |
| **34e** | 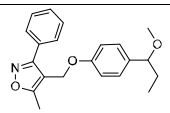 | 95 ± 0.66 | 86 ± 5.0 |

## 4.5 DATA ANALYSIS (PUBLICATION II)

A total of 257 compounds were tested in a GATA4 and NKX2-5 transcriptional synergy assay (**Figure 20**). In addition, the most active compounds were tested in individual assays for inhibition of GATA4 and NKX2-5 and for MTT cell viability assay. The hypothesis was that the assay results of GATA4-NKX2-5 transcriptional synergy, GATA4, NKX2-5, and MTT are not independent of each other. For that reason, data analysis was used to identify dependencies. Furthermore, one of the aims was to identify compounds that potently inhibit transcriptional synergy without inhibiting GATA4.

Interestingly, there was correlation with individual GATA4 and NKX2-5 assays and the synergy assay at 10 μM concentration. NKX2-5 and GATA4 luciferase assay results explained 76% ($r^2$=0.76, **Figure 21A**) and 77% ($r^2$=0.77, **Figure 21C**) of the variation in the transcriptional synergy assay at 10 μM concentration, respectively. The concentration is relatively high and might lead to non-specific effects. At a lower concentration of 3 μM, however, assay readouts explained 64% ($r^2$=0.64, **Figure 21B**) and 53% ($r^2$=0.53, **Figure 21D**) of the variation, respectively, indicating that a concentration of 3 μM is more appropriate for identifying the specific effects of the compounds.

The luciferase assay measures emitting light and it is directly proportional to the amount of living cells, as dead cells do not emit light. For that reason, toxic compounds seem to be active in the assay setting. The cytotoxicity in the MTT assay was measured at the same concentrations and using the same cell line as in the luciferase activity experiments to make results comparable. Cell viabilities of the tested compounds were compared to the results from reporter gene activity of individual GATA4 and NKX2-5 assays at 3 and 10 μM concentrations to test correlations between these results. Compounds were classified as toxic (cell viability <90%, red spots) and nontoxic (cell viability >90%, black spots). In an NKX2-5 assay, cell viability explained 23% ($r^2$=0.23, **Figure 21E**) and 16% ($r^2$=0.16, **Figure 21F**) of the variation for nontoxic compounds at 10 and 3 μM concentrations, respectively. In addition, for toxic compounds there was no significant correlation at 10 and 3 μM concentrations, as cell viability explained 25% ($r^2$=0.25, **Figure 21E**) and 17% ($r^2$=0.17, **Figure 21F**) of the variation, respectively. Interestingly, there is a moderate correlation between the toxic compounds in GATA4 assay and cell viability at 10 and 3 μM concentrations as cell viability explained 69% ($r^2$=0.69, **Figure 21H**) and 42% ($r^2$=0.42, **Figure 21I**) of the variation, respectively.

Next, hierarchical clustering was used to identify compounds that inhibited transcriptional synergy of GATA4 and NKX2-5 without affecting GATA4 gene transcription. Compounds were clustered (**Figure 22**) based on activity in three different assays (NKX2-5, GATA4 and transcriptional synergy assay of GATA4 and NKX2-5). Based on clustering, two interesting groups of compounds were identified at 3 μM concentration: i) compounds which had a relatively similar activity pattern to the original hit compound **1** but did not

inhibit GATA4 (**47d**, **47n**, **SI88**, **39d**); and ii) a group of compounds, which, in addition, did not inhibit NKX2-5 (**3**, **25a**, **47z**, **SI94**, **4f**, **4j**, **SI108**). These two groups of compounds are presented in **Table 8**. Compounds **25a**, **4f**, and **SI108** were excluded from the analysis as they did not inhibit transcriptional synergy at 10 μM concentration, indicating that inhibition at 3 μM concentration was inaccurate in this case.

The most potent synergy inhibitor of these compounds was thiadiazole **47n** (52% of control). Interestingly, isoxazole **47d** with a reversed substitution pattern (compared to the original hit compound **1**) and pyrazole **SI88** also inhibited synergy, although these compounds lacked a methyl substituent in their southern parts. The addition of a fluorine atom to the original hit compound seems to diminish the inhibition of GATA4 (94% of control) in compound **39d**. In addition, the second group of compounds did not inhibit NKX2-5 reporter activity either. This group of compounds consisted of a diverse set of southern parts and contained a bisisoxazole **3**, an imidazole **47z**, a pyrazole **SI94**, and a compound **4j** with a standard southern part and northern part substituted with an ethynyltrimethylsilane moiety.

Finally, compounds that most potently inhibited transcriptional synergy of GATA4 and NKX2-5 at 3 μM concentration were analyzed. The activity data of the eight most potent inhibitors are presented in **Table 9**. The most potent inhibitor of transcriptional synergy at 3 μM concentration was ether derivative **35a** (27% of control). However, it was also cytotoxic (cell viability 76% of control) to cell line (COS-1) used in luciferase assay and for that reason excluded from further research. The next compound, isothiazole **61** had an interesting activity profile as it was only moderately inhibiting GATA4 (71% of control) and potently inhibiting transcriptional synergy (29% of control). Bis-heterocyclic compounds **62** and **47c** also showed potential activity (31% and 45% of control, respectively), although some concerns arose from the cytotoxicity of compound **47c** (cell viability: 85% of control). A nitrothiophene derivative **47u** was a potent inhibitor in all assays, which might indicate some non-specific mechanism of action. N-Acylated secondary amines **58** and **64** were also potent synergy inhibitors, but there were some concerns about cytotoxicity (cell viability: 82 and 85% of control, respectively). Finally, the compound with a reversed substitution pattern in the isoxazole core had an interesting activity pattern, as it was inhibiting transcriptional synergy (42% of control) more than GATA4 (70% of control) and NKX2-5 (68% of control) in reporter gene assays.

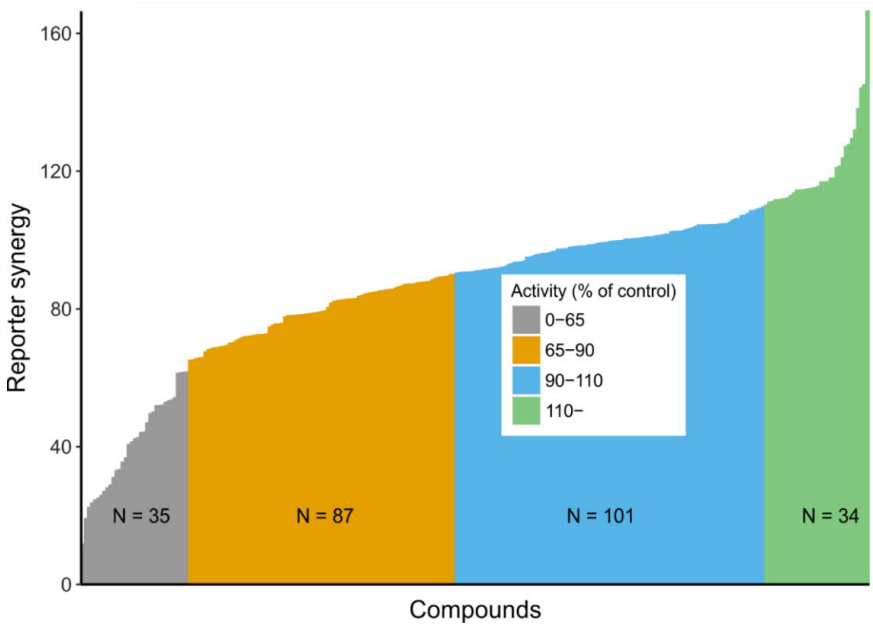


**Figure 20** Reporter synergy of 257 compounds at the concentration of 10 μM. Color codes: gray (0–65% of control), orange (65–90% of control), blue (90–110% of control), and green (110–250% of control).

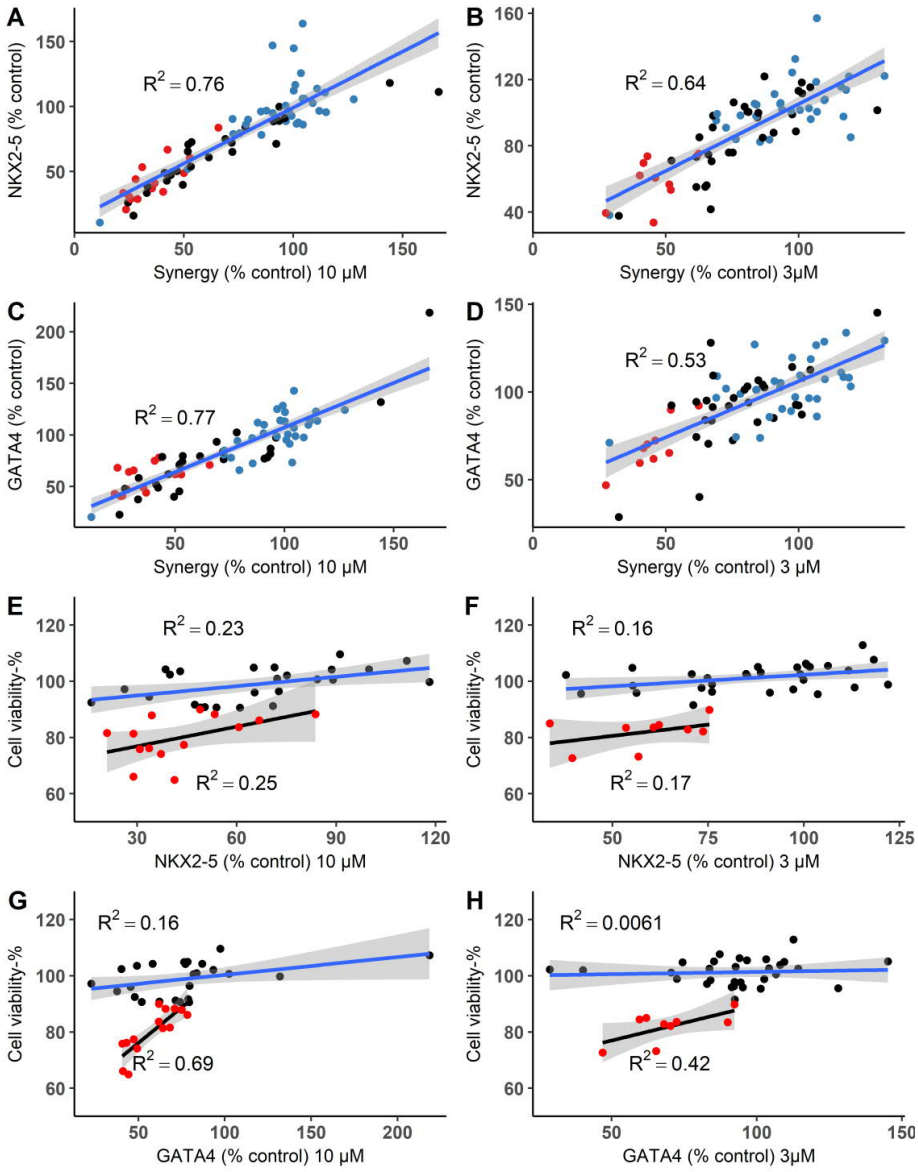


**Figure 21** (A) Relationship of NKX2-5 luciferase reporter gene activity and the transcriptional synergy assay of GATA4 and NKX2-5 at 10 µM concentration; (B) at 3 µM concentration; (C) Relationship of GATA4 luciferase reporter gene activity and the transcriptional synergy assay of GATA4 and NKX2-5 at 10 µM concentration; (D) at 3 µM concentration; (E) Relationship of the NKX2-5 reporter gene activity and cell viability in the MTT assay at 10 µM concentration; (F) at 3 µM concentration; (H) Relationship of GATA4 reporter gene activity and cell viability in the MTT assay at 10 µM concentration; (I) at 3 µM concentration. Red spots: Toxic compounds (cell viability <90% in the respective concentration). Black spots: Nontoxic compounds (cell viability >90% in the respective concentration). Blue spots: Not tested. Blue line (A-D): Linear model for whole data set. Blue line (E-I): Linear model for nontoxic compounds. Black line (E-I): Linear model for toxic compounds. Gray area: 95% confidence interval for linear model predictions.

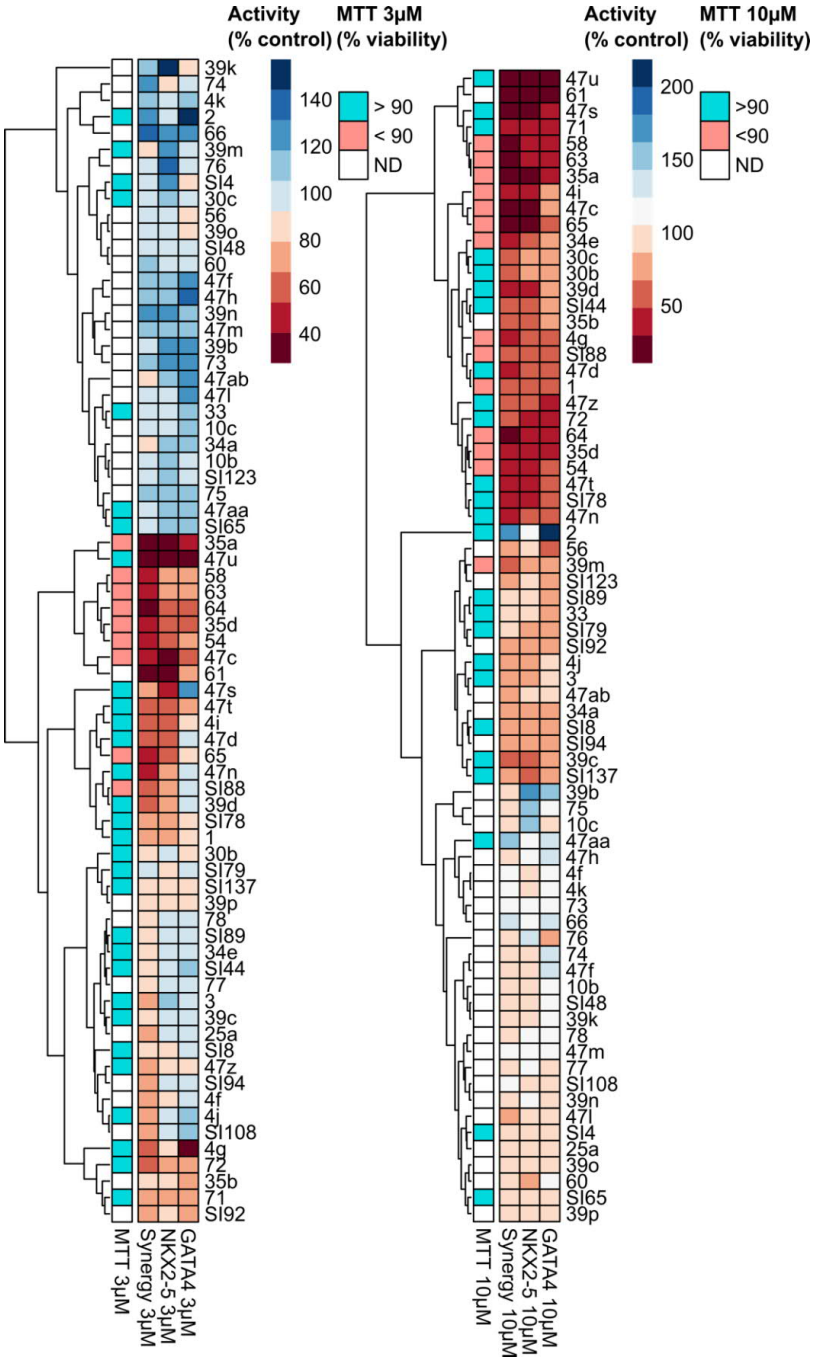


**Figure 22** Hierarchical clustering of the activity data at 3 μM and 10 μM concentrations. Activities of compounds are colored according to the magnitude of inhibition/enhancement. The most potent enhancers are shown in blue and inhibitors in red. Compound numbers are from Publication II.

**Table 8** List of the compounds from hierarchical clustering that inhibit transcriptional synergy of GATA4 and NKX2-5 without affecting GATA4 gene transcription at 3 μM concentration. Compound numbers are from Publication II.

| Cmpd | Structure | Synergy (% of control) Mean ± SD | NKX2-5 (% of control) Mean ± SD | GATA4 (% of control) Mean ± SD |
|---|---|---|---|---|
| **47d** | 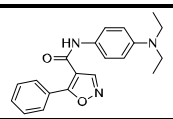 | 65 ± 9.8 | 56 ± 0.01 | 95 ± 15 |
| **47n** | 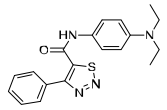 | 52 ± 2.2 | 71 ± 7.7 | 92 ± 6.4 |
| **SI88** | 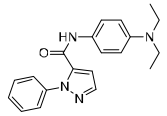 | 62 ± 7.4 | 75 ± 3.4 | 92 ± 5.7 |
| **39d** | 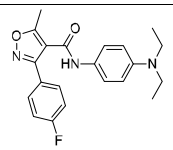 | 61 ± 1.1 | 73 ± 0.8 | 94 ± 22 |
| **3** | 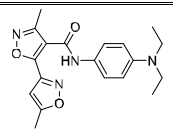 | 76 ± 13 | 106 ± 17 | 97 ± 25 |
| **47z** | 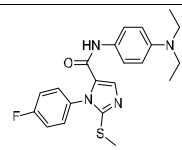 | 68 | 91 ± 5.8 | 91 ± 14 |
| **SI94** | 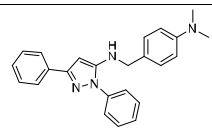 | 69 | 95 ± 11 | 97 ± 18 |
| **4j** | 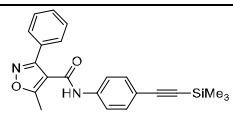 | 68 | 98 ± 0.70 | 110 ± 18 |

**Table 9** List of the most potent GATA4-NKX2-5 transcriptional synergy inhibitors at 3 μM concentration. Compound numbers are from Publication II.

| Cmpd | Structure | Synergy (% of control) Mean ± SD | NKX2-5 (% of control) Mean ± SD | GATA4 (% of control) Mean ± SD |
|---|---|---|---|---|
| **35a** | 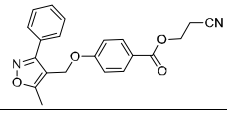 | 27 ± 1.8 | 40 ± 10 | 47 ± 6.5 |
| **61** | 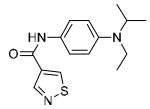 | 29 ± 0.51 | 38 ± 4.4 | 71 ± 5.4 |
| **62** | 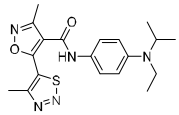 | 31 ± 2.4 | ND | ND |
| **47u** | 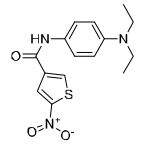 | 32 ± 0.070 | 38 ± 3.9 | 29 ± 4.0 |
| **64** | 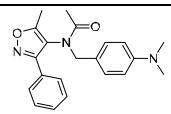 | 40 ± 16 | 62 ± 12 | 60 ± 1.4 |
| **63** | 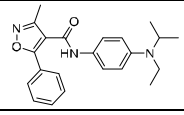 | 42 ± 5.2 | 70 ± 11 | 68 ± 0.8 |
| **58** | 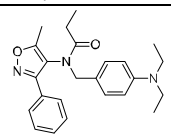 | 43 ± 2.2 | 74 ± 19 | 70 ± 1.1 |
| **47c** | 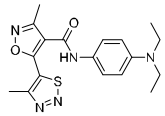 | 45 ± 6.9 | 34 ± 1.2 | 62 ± 19 |

## 4.6 ANTIHYPERTROPHIC ACTIVITY (PUBLICATION II)

B-type natriuretic peptide (BNP) promoter activity is a hypertrophic marker in cardiomyocytes. Hypertrophic gene expression can be induced with endothelin-1 (ET-1). Five compounds (GATA4-NKX2-5 synergy inhibitors **1**, **61**, **47c** and **65**; and the synergy activator **2**) were chosen based on the transcriptional synergy assay data. In the experiment, the cardiomyocytes

were first transfected with a construct containing the -534/+4 proximal region of the rat BNP promoter containing GATA4 and NKX2-5 binding sites in front of luciferase (**Figure 23**). After transfection, compounds were added followed by ET-1 addition 1 h later.

The most potent inhibitor of transcriptional synergy **61** drastically inhibited the BNP promoter activity in cardiomyocytes before and after addition of ET-1. ET-1 induced approximately 3-fold increase in BNP gene activity. Other synergy inhibitors **47c** and **65** showed no statistically significant effect on hypertrophic gene expression. Interestingly, the most potent enhancer of transcriptional synergy, compound **2**, increases hypertrophic gene expression before addition of ET-1. After addition of ET-1, the effect to hypertrophic gene expression diminishes at 10 μM concentration and at 30 μM concentration compound **2** inhibits BNP reporter activity.

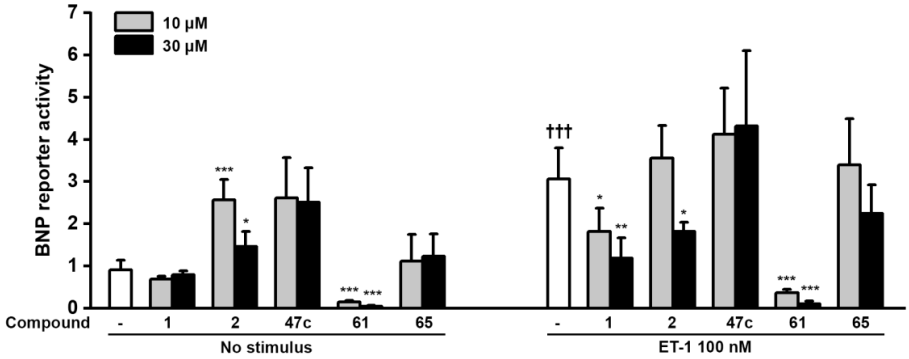


**Figure 23** Hypertrophic BNP gene activation in rat cardiomyocytes with or without ET-1 and the effect of five tested compounds to that. Compound numbers are from Publication II.

## 4.7 TARGET VALIDATION WITH AFFINITY CHROMATOGRAPHY (PUBLICATION III)

Previous study by Välimäki et al.[39] implicated that the original hit compound **1** may bind directly to GATA4, since it decreased phenylephrine-induced GATA4 Ser-105 phosphorylation in cardiomyocytes. The direct binding to GATA4 could prevent protein-protein interaction with NKX2-5 and have antihypertrophic effect in cardiomyocytes.

For affinity chromatography, a compound of interest is immobilized to a solid phase, such as Sepharose® with a linker molecule. Hydrophilic PEG spacer was used as a linker, because it is known to reduce non-specific binding to proteins. The attachment point of the linker molecule has great importance, because critical interactions for compound binding might be lost. The planned attachment points for PEG linker and pegylated derivatives are shown in **Figure 24**. In the SAR study (Chapter 4.3.2), it was noticed that the central amide nitrogen tolerates longer alkyl groups and the northern part tolerates

polar groups or hydrogen bond acceptors. For that reason, those attachment points were chosen for PEG linker. To identify specific targets, an inactive control compound **2** was used. Compound **2** was not active in a transcriptional synergy assay and it lacked a hydrogen bond acceptor next to the isoxazole ring (reversed amide bond compared to the original hit compound **1**).

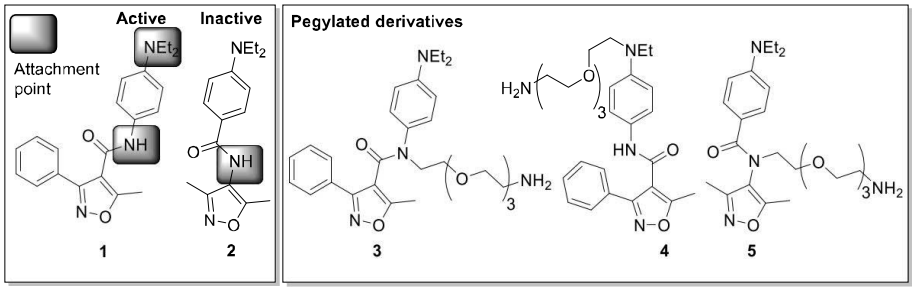


**Figure 24** Attachment points for PEG linker in active (**1**) and inactive (**2**) compounds. Pegylated derivatives of active compound (**3** and **4**) and inactive compound (**5**) for affinity chromatography. Compound numbers are from Publication III.

### 4.7.1 SYNTHESIS

Synthesis of the central part derivatives **3** and **5** started from the alkylation of the amide bonds of compounds **1** and **2** with Boc-$PEG_3$-Br in the presence of KH followed by *tert*-butoxycarbonyl (Boc) removal with a 4 M solution of HCl in 1,4-dioxane (**Scheme 4**). The northern part of derivative **4** was synthesized from *N*-ethyl-4-nitroaniline (**8**). First, *N*-ethyl-4-nitroaniline (**8**) was alkylated with Boc-PEG-Br in the presence of NaH to obtain compound **9**. The nitro group of compound **9** was reduced with palladium-catalyzed hydrogenation to give primary amine **10**. Compound **10** was coupled with 5-methyl-3-phenylisoxazole-4-carboxylic acid. 1-[Bis(dimethylamino)methylene]-1*H*-1,2,3-triazolo[4,5-*b*]pyridinium 3-oxide hexafluorophosphate (HATU) was used as a coupling reagent in a triethylamine-assisted coupling reaction in DMF at room temperature to yield Boc-protected compound **11**. The Boc-group was removed in a 4 M solution of HCl in 1,4-dioxane to give free amine **4**. The free amines **3**-**5** and the sole PEG linker with a methyl end were immobilized to *N*-hydroxysuccinimide-activated Sepharose® in DMF. Successful immobilization was confirmed with Fourier-transform infrared spectroscopy (FTIR).

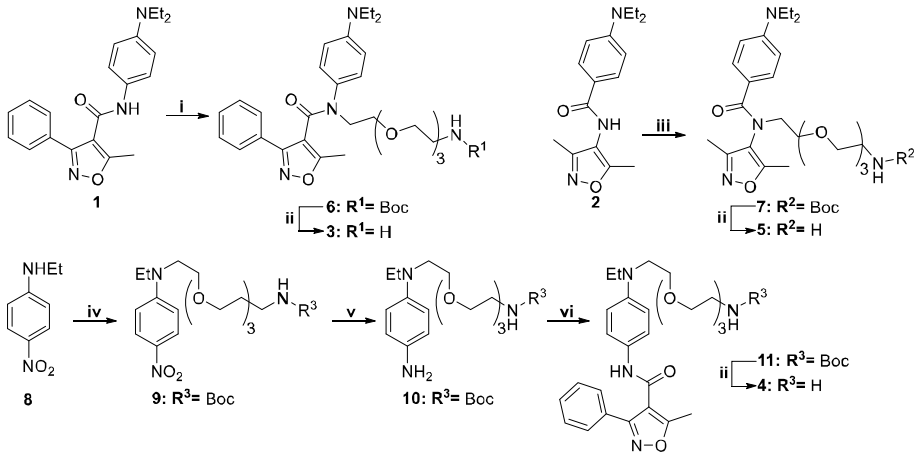


**Scheme 4** Synthesis of pegylated active and inactive compound derivatives. Reagents and conditions: (i) KH (30 w/w %, mineral oil), Boc-$PEG_3$-Br, THF, rt, 2 d; (ii) 4 M HCl in 1,4-dioxane, 0 °C→rt, 2-4 h; (iii) KH (30 w/w %, mineral oil), Boc-$PEG_3$-Br, DMF, rt→80 °C, 72 h; (iv) NaH (60 w/w %, mineral oil), Boc-$PEG_3$-Br, DMF, 0 °C→rt, 1 d; (v) $H_2$, Pd/C, rt, 1 d; (vi) 5-methyl-3-phenylisoxazole-4-carboxylic acid, HATU, $Et_3N$, DMF, rt, 3 d. Compound numbers are from Publication III.

### 4.7.2 BIOLOGICAL TESTING

Immobilized ligands **12**–**15** were used in affinity chromatography to identify if they are binding directly to either GATA4 or NKX2-5 (**Figure 25**). The protocol was modified from the previous study of Kinnunen et al.[99] Proteins of interest (GATA4 and NKX2-5) were overexpressed in COS-1 cells, and the total cell lysate was extracted in protein conformation preserving non-denaturing conditions. This is important for detecting binding in a biologically active conformation. Unbound proteins were washed away from the protein lysate after overnight incubation with the immobilized compound. The bound proteins were released by boiling in SDS sample buffer. The released proteins were resolved by SDS-PAGE and immunoblotted with GATA4 or NKX2-5 antibodies.

According to immunoblotting (**Figure 26**), GATA4 bound to active compounds **14** and **15** but not to the inactive compound **13**. In addition, GATA4 bound mildly to $PEG_3$ linker-containing **12**. On the other hand, NKX2-5 bound almost equally to inactive (**13**) and active (**15**) compound. NKX2-5 bound most potently to $PEG_3$ linker **12** and active compound **14**. As all of the tested compounds bound relatively potently to NKX2-5 it was hypothesized that binding was likely to be non-specific. Binding of active compounds (**14** and **15**) to GATA4 was likely specific, as inactive compound **13** did not bind to GATA4, and $PEG_3$ linker **12** binding was only modest.

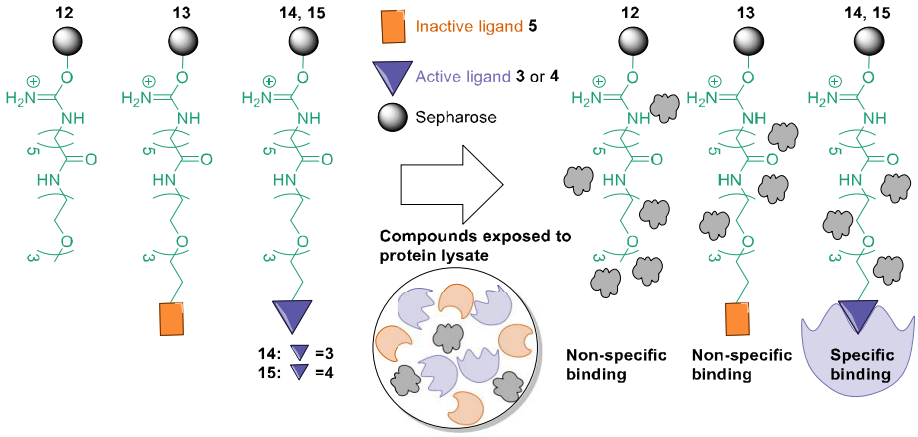


**Figure 25** Schematic illustration of the used affinity chromatography method. Compound numbers are from Publication III.

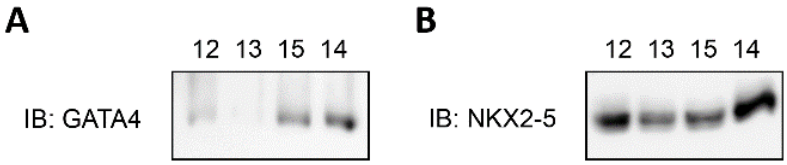


**Figure 26** Western blot images of NKX2-5 or GATA4 binding to immobilized compounds. Protein lysates used in affinity chromatography were either overexpressing GATA4 (A) or NKX2-5 (B). Four different immobilized compounds were used: $PEG_3$ linker **12**, inactive compound **13** or active compounds **14** and **15**. Bound proteins were visualized with either GATA4 or NKX2-5 antibodies. Compound numbers are from Publication III.

# 5 SUMMARY AND CONCLUSIONS

Due to global megatrends, aging populations and population growth, cardiac disease will continue to be the leading cause of death and hospitalization. Transcription factors GATA4 and NKX2-5 are master regulators of cardiac gene expression, taking part in multiple processes regarding heart development, hypertrophy, and recovery after events like myocardial infarction. Hypertrophy is a reversible process of the heart for adaptation to the demands of different physiological conditions, such as normal growth of children, pregnancy, and exercise. Hypertrophic process aims, according to Laplace's law, to reduce wall stress by either increasing the ventricular radius (eccentric hypertrophy) or wall thickness (concentric hypertrophy). However, in pathological conditions, such as long-term hypertension, genetic alterations, and myocardial infarction, this homeostatic process is disrupted. Pathological hypertrophy often leads to cardiac dysfunction, which further progresses to heart failure. Current therapies focus on slowing down the progress of heart failure in pathological conditions, but none of them targets the actual hypertrophic process at a molecular level.

In this thesis design, synthesis and SAR analysis of novel isoxazole-based compounds targeting transcriptional synergy of GATA4-NKX2-5 with antihypertrophic activity are presented. Moreover, binding of the original hit compound **1** directly to GATA4 was validated with affinity chromatography. Furthermore, structural features important for compound activity in transcriptional synergy assays were identified. It was noticed that the hydrogen bond acceptor in the southern part of the compound, corresponding to the nitrogen or oxygen atom of the isoxazole core of the original hit compound **1**, is important for compound activity. Interestingly, sulfur worked equally well as a hydrogen bond acceptor in the position corresponding to the nitrogen or oxygen atom of the isoxazole core. This might be related to thiophene's ability to form intra- or intermolecular noncovalent bonds with π-systems or electron donors with its electron-deficient sulfur's low-lying σ* orbitals of the C–S bond.[100] For the regulation of the specifity of binding, the isoxazole core (in the original hit compound **1**) substituent was found to be important. For synergy inhibition, substitution was not necessary as the most potent compound **61** contained no substituents in the core structure. Compounds that inhibited transcriptional synergy without affecting GATA4 transcriptional activity, all contained either a phenyl or isoxazole ring as a substituent in the southern part of the core ring structure.

In the central part of the compound, amide bond, or other hydrogen bond acceptor, such as ether or N-acylated amine, was a necessary feature for active compounds. However, the free rotation of the central part might increase ethers' and N-acylated amines' susceptibility for the non-specific binding or cytotoxicity.

Furthermore, in the northern part, the active compounds contained either hydrogen bond acceptor(s), donors, or otherwise polar groups. Interestingly, the nitrile-substituted ethers **35a** and **35b** were relatively active, unlike their amide counterparts.

Finally, the mechanism of action of the original hit compound **1** was studied with affinity chromatography. Remarkably, the immobilized hit compound (**1**) bound to GATA4 unlike its inactive counterpart with a missing phenyl substituent in the southern part and reversed amide in the central part.

In conclusion, novel inhibitors of GATA4-NKX2-5 transcriptional synergy were identified, which inhibit hypertrophic gene expression in rat cardiomyocytes. In addition, with hierarchical clustering a group of synergy inhibitors were identified which did not inhibit GATA4 transcriptional activity at 3 μM concentration. Further studies to determine the therapeutic potential of these more selective compounds are clearly needed.

# REFERENCES


(1) Olson, E. Gene Regulatory Networks in the Evolution and Development of the Heart. *Science* **2006**, *313* (5795), 1922–1927.

(2) Puente, B. N.; Kimura, W.; Muralidhar, S. A.; Moon, J.; Amatruda, J. F.; Phelps, K. L.; Grinsfelder, D.; Rothermel, B. A.; Chen, R.; Garcia, J. A.; Santos, C. X.; Thet, S.; Mori, E.; Kinter, M. T.; Rindler, P. M.; Zacchigna, S.; Mukherjee, S.; Chen, D. J.; Mahmoud, A. I.; Giacca, M.; Rabinovitch, P. S.; Aroumougame, A.; Shah, A. M.; Szweda, L. I.; Sadek, H. A. The Oxygen-Rich Postnatal Environment Induces Cardiomyocyte Cell-Cycle Arrest through DNA Damage Response. *Cell* **2014**, *157* (3), 565–579.

(3) Cesna, S.; Eicken, A.; Juenger, H.; Hess, J. Successful Treatment of a Newborn with Acute Myocardial Infarction on the First Day of Life. *Pediatr. Cardiol.* **2013**, *34* (8), 1868–1870.

(4) Saker, D. M.; Walsh-Sukys, M.; Spector, M.; Zahka, K. G. Cardiac Recovery and Survival after Neonatal Myocardial Infarction. *Pediatr. Cardiol.* **1997**, *18* (2), 139–142.

(5) Haubner, B. J.; Schneider, J.; Schweigmann, U.; Schuetz, T.; Dichtl, W.; Velik-Salchner, C.; Stein, J. I.; Penninger, J. M. Functional Recovery of a Human Neonatal Heart after Severe Myocardial Infarction. *Circ. Res.* **2016**, *118* (2), 216–221.

(6) Ma, Y.; Iyer, R. P.; Jung, M.; Czubryt, M. P.; Lindsey, M. L. Cardiac Fibroblast Activation Post-Myocardial Infarction: Current Knowledge Gaps. *Trends Pharmacol. Sci.* **2017**, *38* (5), 448–458.

(7) French, B. A.; Kramer, C. M. Mechanisms of Postinfarct Left Ventricular Remodeling. *Drug Discovery Today: Disease Mechanisms*. 2007.

(8) Flaherty, J. T.; Reid, P. R.; Kelly, D. T.; Taylor, D. R.; Weisfeldt, M. L.; Pitt, B. Intravenous Nitroglycerin in Acute Myocardial Infarction. *Circulation* **1975**, *51* (1), 132–139.

(9) Feldman, R. L.; Pepine, C. J.; Conti, C. R. Magnitude of Dilatation of Large and Small Coronary Arteries by Nitroglycerin. *Circulation* **1981**, *64* (2), 324–333.

(10) Fraccarollo, D.; Galuppo, P.; Hildemann, S.; Christ, M.; Ertl, G.; Bauersachs, J. Additive Improvement of Left Ventricular Remodeling and Neurohormonal Activation by Aldosterone Receptor Blockade with Eplerenone and ACE Inhibition in Rats with Myocardial Infarction. *J. Am. Coll. Cardiol.* **2003**, *42* (9), 1666–1673.

(11) Sayed, D.; He, M.; Yang, Z.; Lin, L.; Abdellatif, M. Transcriptional Regulation Patterns Revealed by High Resolution Chromatin Immunoprecipitation during Cardiac Hypertrophy. *J. Biol. Chem.* **2013**, *288* (4), 2546–2558.

(12) Akazawa, H.; Komuro, I. Roles of Cardiac Transcription Factors in Cardiac Hypertrophy. *Circ. Res.* **2003**, *92* (10), 1079–1088.

(13) Sysak, A.; Obmińska-Mrukowicz, B. Isoxazole Ring as a Useful Scaffold in a Search for New Therapeutic Agents. *Eur. J. Med. Chem.* **2017**, *137*, 292–309.

(14) Grossman, W.; Jones, D.; McLaurin, L. P. Wall Stress and Patterns of

Hypertrophy in the Human Left Ventricle. *J. Clin. Invest.* **1975**, *56* (1), 56–64.
(15) Nakamura, M.; Sadoshima, J. Mechanisms of Physiological and Pathological Cardiac Hypertrophy. *Nat. Rev. Cardiol.* **2018**, *15* (7), 387–407.
(16) Maillet, M.; Van Berlo, J. H.; Molkentin, J. D. Molecular Basis of Physiological Heart Growth: Fundamental Concepts and New Players. *Nat. Rev. Mol. Cell Biol.* **2013**, *14* (1), 38–48.
(17) Vega, R. B.; Konhilas, J. P.; Kelly, D. P.; Leinwand, L. A. Molecular Mechanisms Underlying Cardiac Adaptation to Exercise. *Cell Metab.* **2017**, *25* (5), 1012–1026.
(18) Kim, J.; Wende, A. R.; Sena, S.; Theobald, H. A.; Soto, J.; Sloan, C.; Wayment, B. E.; Litwin, S. E.; Holzenberger, M.; LeRoith, D.; Abel, E. D. Insulin-like Growth Factor I Receptor Signaling Is Required for Exercise-Induced Cardiac Hypertrophy. *Mol. Endocrinol.* **2008**, *22* (11), 2532–2543.
(19) Kinugawa, K.; Jeong, M. Y.; Bristow, M. R.; Long, C. S. Thyroid Hormone Induces Cardiac Myocyte Hypertrophy in a Thyroid Hormone Receptor A1-Specific Manner That Requires TAK1 and P38 Mitogen-Activated Protein Kinase. *Mol. Endocrinol.* **2005**, *19* (6), 1618–1628.
(20) Anderson, B. R.; Granzier, H. L. Titin-Based Tension in the Cardiac Sarcomere: Molecular Origin and Physiological Adaptations. *Prog. Biophys. Mol. Biol.* **2012**, *110* (2–3), 204–217.
(21) Molkentin, J. D. The Transcription Factor C/EBPβ Serves as a Master Regulator of Physiologic Cardiac Hypertrophy. *Circ. Res.* **2011**, *108* (3), 277–278.
(22) Hesse, M.; Welz, A.; Fleischmann, B. K. Heart Regeneration and the Cardiomyocyte Cell Cycle. *Eur. J. Physiol.* **2018**, *470* (2), 241–248.
(23) Eschenhagen, T.; Bolli, R.; Braun, T.; Field, L. J.; Fleischmann, B. K.; Frisén, J.; Giacca, M.; Hare, J. M.; Houser, S.; Lee, R. T.; Marbán, E.; Martin, J. F.; Molkentin, J. D.; Murry, C. E.; Riley, P. R.; Ruiz-Lozano, P.; Sadek, H. A.; Sussman, M. A.; Hill, J. A. Cardiomyocyte Regeneration: A Consensus Statement. *Circulation* **2017**, *136* (7), 680–686.
(24) Van Berlo, J. H.; Kanisicak, O.; Maillet, M.; Vagnozzi, R. J.; Karch, J.; Lin, S. C. J.; Middleton, R. C.; Marbán, E.; Molkentin, J. D. C-Kit + Cells Minimally Contribute Cardiomyocytes to the Heart. *Nature* **2014**, *509* (7500), 337–341.
(25) Boström, P.; Mann, N.; Wu, J.; Quintero, P. A.; Plovie, E. R.; Panáková, D.; Gupta, R. K.; Xiao, C.; MacRae, C. A.; Rosenzweig, A.; Spiegelman, B. M. C/EBPβ Controls Exercise-Induced Cardiac Growth and Protects against Pathological Cardiac Remodeling. *Cell* **2010**, *143* (7), 1072–1083.
(26) Zou, J.; Li, H.; Chen, X.; Zeng, S.; Ye, J.; Zhou, C.; Liu, M.; Zhang, L.; Yu, N.; Gan, X.; Zhou, H.; Xian, Z.; Chen, S.; Liu, P. C/EBPβ Knockdown Protects Cardiomyocytes from Hypertrophy via Inhibition of P65-NFκB. *Mol. Cell. Endocrinol.* **2014**, *390* (1–2), 18–25.
(27) Wilkins, B. J.; Molkentin, J. D. Calcium-Calcineurin Signaling in the Regulation of Cardiac Hypertrophy. *Biochem. Biophys. Res. Commun.* **2004**, *322* (4), 1178–1191.

(28) Rose, B. A.; Force, T.; Wang, Y. Mitogen-Activated Protein Kinase Signaling in the Heart: Angels Versus Demons in a Heart-Breaking Tale. *Physiol. Rev.* **2010**, *90* (4), 1507–1546.
(29) Patient, R. K.; McGhee, J. D. The GATA Family (Vertebrates and Invertebrates). *Curr. Opin. Genet. Dev.* **2002**, *12* (4), 416–422.
(30) Garg, V.; Kathiriya, I. S.; Barnes, R.; Schluterman, M. K.; King, I. N.; Butler, C. A.; Rothrock, C. R.; Eapen, R. S.; Hirayama-Yamada, K.; Joo, K.; Matsuoka, R.; Cohen, J. C.; Srivastava, D. GATA4 Mutations Cause Human Congenital Heart Defects and Reveal an Interaction with TBX5. *Nature* **2003**, *424* (6947), 443–447.
(31) Kohli, S.; Ahuja, S.; Rani, V. Transcription Factors in Heart: Promising Therapeutic Targets in Cardiac Hypertrophy. *Curr. Cardiol. Rev.* **2012**, *7* (4), 262–271.
(32) Durocher, D.; Charron, F. The Cardiac Transcription Factors Nkx2-5 and GATA-4 Are Mutual Cofactors. *EMBO J.* **1997**, *16* (18), 5687–5696.
(33) Pikkarainen, S.; Tokola, H.; Majalahti-Palviainen, T.; Kerkelä, R.; Hautala, N.; Bhalla, S. S.; Charron, F.; Nemer, M.; Vuolteenaho, O.; Ruskoaho, H. GATA-4 Is a Nuclear Mediator of Mechanical Stretch-Activated Hypertrophic Program. *J. Biol. Chem.* **2003**, *278* (26), 23807–23816.
(34) Katanasaka, Y.; Suzuki, H.; Sunagawa, Y.; Hasegawa, K.; Morimoto, T. Regulation of Cardiac Transcription Factor GATA4 by Post-Translational Modification in Cardiomyocyte Hypertrophy and Heart Failure. *Int. Heart J.* **2016**, *57* (6), 672–675.
(35) Vuolteenaho, O.; Ala-Kopsala, M.; Ruskoaho, H. BNP as a Biomarker in Heart Disease. *Adv. Clin. Chem.* **2005**, *40*, 1—36.
(36) Goncalves, G. K.; Caldeira de Oliveira, T. H.; de Oliveira Belo, N. Cardiac Hypertrophy and Brain Natriuretic Peptide Levels in an Ovariectomized Rat Model Fed a High-Fat Diet. *Med. Sci. Monit. Basic Res.* **2017**, *23*, 380–391.
(37) Komuro, I. Molecular Mechanism of Cardiac Hypertrophy and Development. *Jpn. Circ. J.* **2001**, *65* (5), 353–358.
(38) Kinnunen, S.; Välimäki, M.; Tölli, M.; Wohlfahrt, G.; Darwich, R.; Komati, H.; Nemer, M.; Ruskoaho, H. Nuclear Receptor-Like Structure and Interaction of Congenital Heart Disease-Associated Factors GATA4 and NKX2-5. *PLoS One* **2015**, *10* (12), e0144145.
(39) Välimäki, M. J.; Tölli, M. A.; Kinnunen, S. M.; Aro, J.; Serpi, R.; Pohjolainen, L.; Talman, V.; Poso, A.; Ruskoaho, H. J. Discovery of Small Molecules Targeting the Synergy of Cardiac Transcription Factors GATA4 and NKX2-5. *J. Med. Chem.* **2017**, *60* (18), 7781–7798.
(40) Talley, J. J.; Brown, D. L.; Carter, J. S.; Graneto, M. J.; Koboldt, C. M.; Masferrer, J. L.; Perkins, W. E.; Rogers, R. S.; Shaffer, A. F.; Zhang, Y. Y.; Zweifel, B. S.; Seibert, K. 4-[5-Methyl-3-phenylisoxazol-4-yl]-Benzenesulfonamide, Valdecoxib : A Potent and Selective Inhibitor of COX-2. *J. Med. Chem.* **2000**, *43*, 775–777.
(41) Liu, B.; Liu, G.; Xin, Z.; Serby, M. D.; Zhao, H.; Schaefer, V. G.; Falls, H. D.; Kaszubska, W.; Collins, C. a.; Sham, H. L. Novel Isoxazole Carboxamides as Growth Hormone Secretagogue Receptor (GHS-R) Antagonists. *Bioorg. Med. Chem. Lett.* **2004**, *14* (20), 5223–5226.
(42) Bartlett, R. R.; Schleyerbach, R. Immunopharmacological Profile of a

Novel Isoxazol Derivative, HWA 486, with Potential Antirheumatic Activity - I. Disease Modifying Action on Adjuvant Arthritis of the Rat. *Int. J. Immunopharmacol.* **1985**.
(43) Davis, J. P.; Cain, G. a.; Pitts, W. J.; Magolda, R. L.; Copeland, R. a. The Immunosuppressive Metabolite of Leflunomide Is a Potent Inhibitor of Human Dihydroorotate Dehydrogenase. *Biochemistry* **1996**, *35* (4), 1270–1273.
(44) Bamborough, P.; Diallo, H.; Goodacre, J. D.; Gordon, L.; Lewis, A.; Seal, J. T.; Wilson, D. M.; Woodrow, M. D.; Chung, C. W. Fragment-Based Discovery of Bromodomain Inhibitors Part 2: Optimization of Phenylisoxazole Sulfonamides. *J. Med. Chem.* **2012**, *55* (2), 587–596.
(45) Hu, F.; Szostak, M. Recent Developments in the Synthesis and Reactivity of Isoxazoles: Metal Catalysis and Beyond. *Adv. Synth. Catal.* **2015**, *357* (12), 2583–2614.
(46) Quilico, A.; D'Alcontres, G. Stagno; Grünanger, P. A New Reaction of Ethylenic Double Bonds. *Nature* **1950**, *166* (4214), 226–227.
(47) Quilico, A.; Speroni, G. Sintesi Di Derivati Del l'ìsossazolo Con l'acido Fulminico. Nota I. *Gazz. Chim. Ital.* **1939**, *69*, 508–535.
(48) Fukui, K.; Yonezawa, T.; Shingu, H. A Molecular Orbital Theory of Reactivity in Aromatic Hydrocarbons. *J. Chem. Phys.* **1952**, *20* (4), 722–725.
(49) Sustmann, R.; Trill, H. Substituent Effects in 1,3-Dipolar Cycloadditions of Phenyl Azide. *Angew. Chem., Int. Ed. Engl.* **1972**, *11* (9), 838–840.
(50) Huisgen, R.; Szeimies, G.; Möbius, L. 1.3-Dipolare Cycloadditionen, XXXII. Kinetik Der Additionen Organischer Azide an CC-Mehrfachbindungen. *Chem. Ber.* **1967**, *100* (8), 2494–2507.
(51) Houk, K. N.; Sims, J.; Watts, C. R.; Luskus, L. J. Origin of Reactivity, Regioselectivity, and Periselectivity In 1,3-Dipolar Cycloadditions. *J. Am. Chem. Soc.* **1973**, *95* (22), 7301–7315.
(52) Sustmann, R. Orbital Energy Control of Cycloaddition. *Pure Appl. Chem.* **1974**, *40* (4), 569–593.
(53) Hu, Y.; Houk, K. N. Quantitative Predictions of Substituent and Solvent Effects on the Regioselectivities of Nitrile Oxide Cycloadditions to Electron-Deficient Alkynes. *Tetrahedron* **2000**, *56* (42), 8239–8243.
(54) Sobhi, C.; Nacereddine, A. K.; Nasri, L.; Lechtar, Z.; Djerourou, A. A DFT Study of the Mechanism and the Regioselectivity of [3 + 2] Cycloaddition Reactions of Nitrile Oxides with α,β-Acetylenic Aldehyde. *Mol. Phys.* **2016**, *114* (21), 3193–3200.
(55) Yoshimura, A.; Middleton, K. R.; Todora, A. D.; Kastern, B. J.; Koski, S. R.; Maskaev, A. V.; Zhdankin, V. V. Hypervalent Iodine Catalyzed Generation of Nitrile Oxides from Oximes and Their Cycloaddition with Alkenes or Alkynes. *Org. Lett.* **2013**, *15* (15), 4010–4013.
(56) Singhal, A.; Kumar, S.; Parumala, R.; Sharma, A.; Peddinti, R. K. Hypervalent Iodine Mediated Synthesis of Di- and Tri-Substituted Isoxazoles via [3+2] Cycloaddition of Nitrile Oxides. *Tetrahedron Lett.* **2015**, *57* (7), 719–722.
(57) Han, L.; Zhang, B.; Zhu, M.; Yan, J. An Environmentally Benign Synthesis of Isoxazolines and Isoxazoles Mediated by Potassium Chloride in Water. *Tetrahedron Lett.* **2014**, *55* (14), 2308–2311.
(58) Liu, K.; Shelton, B. R.; Howe, R. K. A Particularly Convenient

Preparation of Benzohydroximinoyl Chlorides (Nitrile Oxide Precursors). *J. Org. Chem.* **1980**, *45* (19), 3916–3918.
(59) Huisgen, R. 1,3-Dipolar Cycloadditions Past and Future. *Angew. Chem., Int. Ed. Engl.* **1963**, *2* (10), 565–632.
(60) Kesornpun, C.; Aree, T.; Mahidol, C.; Ruchirawat, S.; Kittakoop, P. Corrigendum to: Water-Assisted Nitrile Oxide Cycloadditions: Synthesis of Isoxazoles and Stereoselective Syntheses of Isoxazolines and 1,2,4-Oxadiazoles *Angew. Chem., Int. Ed. Engl.* **2016**, *55* (36), 10548.
(61) Grecian, S.; Fokin, V. V. Ruthenium-Catalyzed Cycloaddition of Nitrile Oxides and Alkynes: Practical Synthesis of Isoxazoles. *Angew. Chem., Int. Ed. Engl.* **2008**, *47* (43), 8285–8287.
(62) She, Z.; Niu, D.; Chen, L.; Gunawan, M. A.; Shanja, X.; Hersh, W. H.; Chen, Y. Synthesis of Trisubstituted Isoxazoles by Palladium(II)-Catalyzed Cascade Cyclization-Alkenylation of 2-Alkyn-1-one *O*-Methyl Oximes. *J. Org. Chem.* **2012**, *77* (7), 3627–3633.
(63) Himo, F.; Lovell, T.; Hilgraf, R.; Rostovtsev, V. V.; Noodleman, L.; Sharpless, K. B.; Fokin, V. V. Copper(I)-Catalyzed Synthesis of Azoles. DFT Study Predicts Unprecedented Reactivity and Intermediates. *J. Am. Chem. Soc.* **2005**, *127* (1), 210–216.
(64) Aldeghi, M.; Malhotra, S.; Selwood, D. L.; Chan, A. W. E. Two- and Three-Dimensional Rings in Drugs. *Chem. Biol. Drug Des.* **2014**, *83* (4), 450–461.
(65) Taylor, R. D.; Maccoss, M.; Lawson, A. D. G. Rings in Drugs. *J. Med. Chem.* **2014**, *57* (14), 5845–5859.
(66) Kalgutkar, A.; Gardner, I.; Obach, R.; Shaffer, C.; Callegari, E.; Henne, K.; Mutlib, A.; Dalvie, D.; Lee, J.; Nakai, Y.; O'Donnell, J.; Boer, J.; Harriman, S. A Comprehensive Listing of Bioactivation Pathways of Organic Functional Groups. *Curr. Drug Metab.* **2005**, *6* (3), 161–225.
(67) Munde, M.; Lee, M.; Neidle, S.; Arafa, R.; Boykin, D. W.; Liu, Y.; Bailly, C.; Wilson, W. D. Induced Fit Conformational Changes of a "Reversed Amidine" Heterocycle: Optimized Interactions in a DNA Minor Groove Complex. *J. Am. Chem. Soc.* **2007**, *129* (17), 5688–5698.
(68) Rydberg, P.; Vasanthanathan, P.; Oostenbrink, C.; Olsen, L. Fast Prediction of Cytochrome P450 Mediated Drug Metabolism. *ChemMedChem* **2009**, *4* (12), 2070–2079.
(69) Peterson, L. a. Reactive Metabolites in the Biotransformation of Molecules Containing a Furan Ring. *Chem. Res. Toxicol.* **2013**, *26* (1), 6–25.
(70) Guengerich, F. P. Cytochrome P450 Oxidations in the Generation of Reactive Electrophiles: Epoxidation and Related Reactions. *Arch. Biochem. Biophys.* **2003**, *409* (1), 59–71.
(71) V Ravindranath, LT Burka, M. B. Reactive Metabolites from the Bioactivation of Toxic Methylfurans. *Science* **1984**, *224* (4651), 884–886.
(72) Shaik, S.; Kumar, D.; de Visser, S. P.; Altun, A.; Thiel, W. Theoretical Perspective on the Structure and Mechanism of Cytochrome P450 Enzymes. *Chem. Rev.* **2005**, *105* (6), 2279–2328.
(73) Waters, M. L. Aromatic Interactions in Model Systems. *Curr. Opin. Chem. Biol.* **2002**, *6* (6), 736–741.

(74) Soni, A.; Khurana, P.; Singh, T.; Jayaram, B. A DNA Intercalation Methodology for an Efficient Prediction of Ligand Binding Pose and Energetics. *Bioinformatics* **2017**, *33* (10), 1488–1496.
(75) Martinez, C. R.; Iverson, B. L. Rethinking the Term "Pi-Stacking." *Chem. Sci.* **2012**, *3* (7), 2191–2201.
(76) Bootsma, A. N.; Wheeler, S. E. Converting SMILES to Stacking Interaction Energies. *J. Chem. Inf. Model.* **2019**, *59* (8), 3413–3421.
(77) Liu, F.; Zhang, Z.; Levit, A.; Levring, J.; Touhara, K. K.; Shoichet, B. K.; Chen, J. Structural Identification of a Hotspot on CFTR for Potentiation. *Science* **2019**, *364* (6446), 1184–1188.
(78) Rose, A. S.; Bradley, A. R.; Valasatava, Y.; Duarte, J. M.; Prlić, A.; Rose, P. W. NGL Viewer: Web-Based Molecular Graphics for Large Complexes. *Bioinformatics* **2018**, *34* (21), 3755–3758.
(79) Hurley, L. H. DNA and Its Associated Processes as Targets for Cancer Therapy. *Nat. Rev. Cancer* **2002**, *2* (3), 188–200.
(80) Lerman, L. S. Structural Considerations in the Interaction of DNA and Acridines. *J. Mol. Biol.* **1961**, *3* (1), 18–30.
(81) Neidle, S.; Jones, T. A. Crystal Structure of Proflavine, a DNA Binding Agent. *Nature* **1975**, *253* (5489), 284–285.
(82) Torigoe, H.; Sato, S.; Yamashita, K. ichi; Obika, S.; Imanishi, T.; Takenaka, S. Binding of Threading Intercalator to Nucleic Acids: Thermodynamic Analyses. *Nucleic Acids Res. Suppl.* **2002**, No. 2, 55–56.
(83) Chung-Hang Leung, Daniel Shiu-Hin Chan, Victor Pui-Yan Ma, D.-L. M. DNA-Binding SmallMolecules as Inhibitors OfTranscription Factors Chung-Hang. *Med. Res. Rev.* **2013**, *33* (4), 823–846.
(84) Lee, J. A.; Eder, J.; Vincent, F.; Prunotto, M.; Moffat, J. G. Opportunities and Challenges in Phenotypic Drug Discovery: An Industry Perspective. *Nat. Rev. Drug Discov.* **2017**, *16* (8), 531–543.
(85) Cuatrecasas, P. Protein Purification by Affinity Chromatography. *J. Biol. Chem.* **1970**, *245* (12), 3059.
(86) Depeursinge, A.; Racoceanu, D.; Iavindrasana, J.; Cohen, G.; Platon, A.; Poletti, P.-A.; Muller, H. Identification of a Novel Protein Regulating Microtubule Stability through a Chemical Approach. *Artif. Intell. Med.* **2010**, *11*, 1118.
(87) He, G.; Luo, W.; Li, P.; Remmers, C.; Netzer, W. J.; Hendrick, J.; Bettayeb, K.; Flajolet, M.; Gorelick, F.; Wennogle, L. P.; Greengard, P. Gamma-Secretase Activating Protein Is a Therapeutic Target for Alzheimer's Disease. *Nature* **2010**, *467* (7311), 95–98.
(88) Knockaert, M.; Lenormand, P.; Gray, N.; Schultz, P.; Pouysségur, J.; Meijer, L. P42/P44 MAPKs Are Intracellular Targets of the CDK Inhibitor Purvalanol. *Oncogene* **2002**, *21* (42), 6413–6424.
(89) Bach, S.; Knockaert, M.; Reinhardt, J.; Lozach, O.; Schmitt, S.; Baratte, B.; Koken, M.; Coburn, S. P.; Tang, L.; Jiang, T.; Liang, D. C.; Galons, H.; Dierick, J. F.; Pinna, L. A.; Meggio, F.; Totzke, F.; Schächtele, C.; Lerman, A. S.; Carnero, A.; Wan, Y.; Gray, N.; Meijer, L. Roscovitine Targets, Protein Kinases and Pyridoxal Kinase. *J. Biol. Chem.* **2005**, *280* (35), 31208–31219.
(90) Ito, T.; Ando, H.; Suzuki, T.; Ogura, T.; Hotta, K.; Imamura, Y.; Yamaguchi, Y.; Handa, H. Identification of a Primary Target of

Thalidomide Teratogenicity. *Science* **2010**, *327* (5971), 1345–1350.
(91) Koteva, K.; Hong, H. J.; Wang, X. D.; Nazi, I.; Hughes, D.; Naldrett, M. J.; Buttner, M. J.; Wright, G. D. A Vancomycin Photoprobe Identifies the Histidine Kinase VanSsc as a Vancomycin Receptor. *Nat. Chem. Biol.* **2010**, *6* (5), 327–329.
(92) Ziegler, S.; Pries, V.; Hedberg, C.; Waldmann, H. Target Identification for Small Bioactive Molecules: Finding the Needle in the Haystack. *Angew. Chem., Int. Ed. Engl.* **2013**, *52* (10), 2744–2792.
(93) Zheng, W.; Li, G.; Li, X. Affinity Purification in Target Identification: The Specificity Challenge. *Arch. Pharm. Res.* **2015**, *38* (9), 1661–1685.
(94) Oda, Y.; Owa, T.; Sato, T.; Boucher, B.; Daniels, S.; Yamanaka, H.; Shinohara, Y.; Yokoi, A.; Kuromitsu, J.; Nagasu, T. Quantitative Chemical Proteomics for Identifying Candidate Drug Targets. *Anal. Chem.* **2003**, *75* (9), 2159–2165.
(95) Huisgen, R. Kinetics and Mechanism of 1,3-Dipolar Cycloadditions. *Angew. Chem., Int. Ed. Engl.* **1963**, *2* (11), 633–645.
(96) Butler, R. N.; Coyne, A. G. Water: Nature's Reaction Enforcer-Comparative Effects for Organic Synthesis "in-Water" and "on-Water." *Chem. Rev.* **2010**, *110* (10), 6302–6337.
(97) Gholami, M. R.; Habibi Yangjeh, A. Kinetics of 1, 3-Dipolar Cycloaddition Reaction between C, N-Diphenylnitrone and Dimethyl Fumarate in Various Solvents and Aqueous Solutions. *Int. J. Chem. Kinet.* **2000**, 32 (7), 431–434.
(98) Shinada, N. K.; De Brevern, A. G.; Schmidtke, P. Halogens in Protein-Ligand Binding Mechanism: A Structural Perspective. *J. Med. Chem.* **2019**.
(99) Kinnunen, S. M.; Tölli, M.; Välimäki, M. J.; Gao, E.; Szabo, Z.; Rysä, J.; Ferreira, M. P. A.; Ohukainen, P.; Serpi, R.; Correia, A.; Mäkilä, E.; Salonen, J.; Hirvonen, J.; Santos, H. A.; Ruskoaho, H. Cardiac Actions of a Small Molecule Inhibitor Targeting GATA4–NKX2-5 Interaction. *Sci. Rep.* **2018**, *8* (1), 4611.
(100) Beno, B. R.; Yeung, K.-S.; Bartberger, M. D.; Pennington, L. D.; Meanwell, N. a. A Survey of the Role of Noncovalent Sulfur Interactions in Drug Design. *J. Med. Chem.* **2015**, *58* (11), 4383–4438.

ISBN 978-951-51-6181-9 (PRINT)
ISBN 978-951-51-6182-6 (ONLINE)
ISSN 2342-3161 (PRINT)
ISSN 2342-317X (ONLINE)
http://ethesis.helsinki.fi

HELSINKI 2020